NASA Technical Memorandum 81947

Description of Recent Changes in the Langley 6- by 28-Inch Transonic Tunnel

William G. Sewall

MAY 1981

NASA

Description of Recent Changes in the Langley 6- by 28-Inch Transonic Tunnel

William G. Sewall
Langley Research Center
Hampton, Virginia

SUMMARY

The Langley 6- by 28-Inch Transonic Tunnel is a two-dimensional blowdown tunnel with slotted top and bottom walls and is used primarily for testing airfoil sections. Using available theory, the top and bottom slotted walls were redesigned for minimum wind-tunnel interference errors of blockage and streamline curvature. To minimize Mach number gradients along the tunnel axis downstream of the model, controllable flaps were installed to regulate the flow reentering the test section through the slotted walls. The flap setting is independent of stagnation pressure and varies only with Mach number. The freestream Mach number is determined from the pressure measured at a station 66.04 cm (26.00 in.) upstream of the model station. The model has no significant influence on the vertical Mach number distribution at this station. This method of Mach number determination appears to be more accurate than one using the plenum pressure.

INTRODUCTION

The Langley 6- by 28-Inch Transonic Tunnel is a two-dimensional blowdown tunnel used primarily for testing airfoils at moderate Reynolds numbers with independent control of both Mach number and stagnation pressure. The models normally used in most airfoil tests have a 15.24 cm (6.00 in.) chord which allows a constant Reynolds number based on model chord of the order of 10×10^6 for Mach numbers between 0.5 and 1.0. Usually, the Mach numbers range from $M = 0.3$ to $M = 0.95$, and stagnation pressures vary from 207 kPa (30 lb/in^2) to 620 kPa (90 lb/in^2) resulting in Reynolds numbers from 2.0×10^6 to 14.0×10^6.

The Langley 6- by 28-Inch Transonic Tunnel was designed in 1968 to replace the former Langley 20-Inch Variable Supersonic Tunnel which was operational from 1957 to 1965. The 20-Inch Variable Supersonic Tunnel was a horizontal facility mounted above the Langley 26-Inch Transonic Blowdown Tunnel. The settling chambers of these two facilities were interconnected through an isolation valve and piping manifold so that both could make use of a common air supply to regulate tunnel stagnation pressure. The 20-Inch Variable Supersonic Tunnel was chosen for replacement because it had not been operational for several years and much of the existing hardware could be utilized for the 6- by 28-Inch Tunnel.

The 6- by 28-Inch Transonic Tunnel first became operational in late 1974 with the first test consisting of tunnel-empty surveys of sidewall Mach number, noise, and test-section total pressure as described in reference 1. The original test section of the tunnel had slotted top and bottom walls with an openness ratio of 12.5 percent which were used for tests of approximately 20 airfoils, including a supercritical airfoil.

In late 1976, after reviewing both airfoil and tunnel-empty test data and studying slotted-wall theory, two problems became apparent in the original test

section. First, the openness ratio of the slotted wall appeared excessive according to the theory presented in reference 2. The second problem was an unfavorable tunnel-empty sidewall Mach number distribution in the region of the test section downstream of the model station.

The problem of excessive openness ratio was alleviated by reducing the openness ratio from 12.5 percent to 5.0 percent and increasing the slot spacing from 3.81 cm (1.50 in.) to 15.24 cm (6.00 in.). This modification, according to available data analysis, offered minimum blockage and lift interference.

The Mach number distribution was improved by extending the slotted walls farther downstream of the model station and adding controllable flaps to regulate the air reentering the test section downstream of the model.

This paper presents a description of the modified slotted wall and the controllable flaps. Settings for the controllable flaps are determined so that acceptable tunnel-empty sidewall Mach number distributions occur in the test-section region downstream of the model station. In addition, this paper presents a comparison in free-stream Mach number determination between using the pressure in the plenum chamber surrounding the test section and using a pressure on the test-section sidewall upstream of the model station. The free-stream Mach number calibration is also presented in this paper.

SYMBOLS

The units used for the physical quantities of this paper are given in both the International System of Units (SI) and in the U.S. Customary Units. The measurements and calculations were made in the U.S. Customary Units.

c_p static pressure coefficient, $\dfrac{p_{local} - p_\infty}{q_\infty}$

$c_{p,sonic}$ static pressure coefficient where $M_{local} = 1.00$, $\dfrac{(0.5283 - p_\infty/p_{t,\infty})p_{t,\infty}}{q_\infty}$

c airfoil chord, cm (in.)

c_d section profile-drag coefficient, $\displaystyle\sum_{Wake} c_d' \, \frac{\Delta h}{c}$

c_d' point drag coefficient,

$$2\left(\frac{p_w}{p_\infty}\right)^{6/7}\left[\frac{\left(\frac{p_{t,w}}{p_w}\right)^{2/7} - 1}{\left(\frac{p_{t,\infty}}{p_\infty}\right)^{2/7} - 1}\right]^{1/2}\left\{\left(\frac{p_{t,w}}{p_{t,\infty}}\right)^{1/7} - \left[\frac{\left(\frac{p_{t,w}}{p_\infty}\right)^{2/7} - 1}{\left(\frac{p_{t,\infty}}{p_\infty}\right)^{2/7} - 1}\right]^{1/2}\right\}$$

c_m section pitching-moment coefficient about quarter chord,

$$\sum_{\substack{\text{Upper} \\ \text{surface}}} c_p\left(0.25 - \frac{x}{c}\right)\frac{\Delta x}{c} + \sum_{\substack{\text{Lower} \\ \text{surface}}} c_p\left(0.25 - \frac{x}{c}\right)\frac{\Delta x}{c}$$

c_n section normal-force coefficient, $\displaystyle\sum_{\substack{\text{Upper} \\ \text{surface}}} c_p\frac{\Delta x}{c} + \sum_{\substack{\text{Lower} \\ \text{surface}}} c_p\frac{\Delta x}{c}$

h semiheight of test section, cm (in.)

M_{local} local Mach number at position on either model or tunnel sidewall calculated from measured local pressure

M_{TC} test-chamber Mach number calculated from p_{TC} and $p_{t,\infty}$

$$\left\{5\left[\left(\frac{p_{t,\infty}}{p_{TC}}\right)^{2/7} - 1\right]\right\}^{1/2}$$

M_{US} Mach number at upstream station $x = -66.04$ cm $(-26.00$ in.)

M_∞ free-stream Mach number determined from M_{TC}

M_∞' free-stream Mach number determined from M_{US}

P_{local} local pressure at position on model or tunnel

p_{TC} static pressure measured in test-section plenum chamber, kPa (psia)

$p_{t,w}$ total pressure measured on traversing survey probe, kPa (psia)

$p_{t,\infty}$ free-stream stagnation pressure or total pressure, kPa (psia)

3

p_w static pressure measured on tunnel sidewall near traversing survey probe, kPa (psia)

p_∞ free-stream static pressure, kPa (psia)

q_∞ free-stream dynamic pressure, kPa (psia)

R   Reynolds number based on model chord

T_t stagnation temperature, $^\circ R$

x   distance along longitudinal axis measured from model station, positive downstream and negative upstream of model station, cm (in.)

z   distance along vertical axis measured from longitudinal axis, positive above and negative below longitudinal axis, cm (in.)

α angle of attack, deg

GENERAL DESCRIPTION

The Langley 6- by 28-Inch Transonic Tunnel, a two-dimensional facility with solid sidewalls and slotted top and bottom walls, operates on direct blowdown from a supply of dry compressed air. A photograph of the facility, taken during the assembly of the tunnel, is shown in figure 1. A drawing of the facility is shown in figure 2 which indicates the portion of the facility that was replaced to provide for the two-dimensional test section. The physical relationship and interconnecting piping between this facility and the 26-Inch Transonic Blowdown Tunnel are evident in both of these figures. The dry compressed air is routed through the interconnecting piping to the 6- by 28-Inch Transonic Tunnel as described in reference 1.

A cross-section drawing of the entrance section, test section, downstream transition section, and enclosing pressure shell is presented in figure 3. The pressure shell, which forms the test-section plenum chamber referred to as the test chamber is cylindrical with a length of 380.49 cm (149.80 in.) and an inside diameter of 193.04 cm (76.00 in.). The rectangular test section begins at station -96.52 cm (-38.00 in.) and ends at station 112.40 cm (44.25 in.). Two turntables with a diameter of 24.13 cm (9.50 in.) are located in the sidewalls and provide model support. The center line of the turntables is located at station 0.0. The test section has constant height and width throughout its length.

Slotted Walls

The present slotted walls are shown in figure 3(b) which also shows the original slotted walls. The present slotted walls consist of four longitudinal half slots along the junction of the floor and ceiling and the tunnel sidewalls. These half slots begin at station -91.44 cm (-36.00 in.) and widen uniformly to

4

0.38 cm (0.15 in.) at station -66.04 cm (-26.00 in.) where slot width remains constant, forming the 5.0 percent openness ratio through the model station to the end of the slotted walls at station 97.79 cm (38.50 in.).

The floor and ceiling are formed by two plates pinned together at the wall center line to maintain a smooth butt joint, as shown in figure 3(c). Two 0.95-cm (0.373-in.) thick bars, the strongback stiffeners, are attached to each plate outside of the airstream surface, as shown in figure 3(c). These strong-back stiffeners run parallel down the full length of the plates and are joined together by spacers to provide structural support for the slotted walls. Figure 3(d) shows the attachment of the upstream and downstream ends of the slotted walls to the test section. The upstream end of the slotted wall is held to the entrance section by the end splice (fig. 3(d)) and the downstream end is fixed with the pin support (fig. 3(d)). The midsection of the slotted walls is anchored by the support rod at tunnel station 13.97 cm (5.50 in.). With the pin support anchoring the downstream end and the support rod holding the mid-section, the slotted walls are fixed parallel to the tunnel axis, as are the sidewalls.

Flaps

Air which has passed through the slotted walls into the test chamber is returned to the airstream over controllable flaps located inside of the reen-trant flow fairings, as indicated in figure 3(a). The reentrant flow fairings begin at tunnel station 27.31 cm (10.75 in.), and the flap is a hinged plate pivoting at tunnel station 32.38 cm (12.75 in.), 18.03 cm (7.10 in.) above the slotted wall. Figure 3(e) shows the details of the flap looking upstream from the end of the flap. The end of the flap is cut out to provide space for the strongback stiffeners so that when the flap is fully closed, the end of the flap touches the outside edge of the slotted wall at tunnel station 87.12 cm (34.30 in.). In the fully open position, there is a 4.01 cm (1.58 in.) gap between the end of the flap and the outside surface of the slotted wall. A small electric servomotor controls flap position by rotating the receiver piece as shown in figure 3(e). This receiver piece regulates the exposed length of the threaded clevis that is connected to the flap. A potentiometer is geared to the servomotor to show flap position at the control console. The flap posi-tion is controllable to within ±0.02 cm (±0.01 in.) vertical distance at the end of the flap toward the outside surface of the slotted walls.

Mach Number Control

Mach number is controlled by two sliding choker doors at tunnel station 112.40 cm (44.25 in.) as shown in figure 3(a). The Mach number ranges between 0.3 and 1.2. The two doors extend the full height of the tunnel and are inserted into the airstream by means of a hydraulic control system. When inserted, these doors create a local minimum cross-section area and thus cause sonic velocity at the choker door location. The Mach number in the test sec-tion upstream of the choker doors can be controlled by the amount of area reduc-tion by the doors.

Transition Section and Diffuser

A transition section is located downstream of the choker door which provides a linear increase in cross-section area from the test section of the 6- by 28-Inch Tunnel to the existing 20-inch-square-cross-section second minimum and conical diffuser of the previous supersonic tunnel installation. The air is exhausted to the atmosphere through a vertical stack (fig. 2) which has sound attenuation baffles.

Control Systems

The facility has four independent primary control systems: a valve control system for maintaining stagnation pressure while the tank supply pressure decreases, a choker door system for Mach number control, a test-section turntable rotation system for model angle of attack, and a flap drive system to control flap position. The first three systems use closed-loop hydraulic servovalves for operation, while the fourth system, the flap control system, is manually set using a potentiometer readout with the electric motor drive system. The controls are located on a console in the control room which is shown in figure 4. Real-time displays of tunnel parameters are provided on this panel. The analog set points for the control systems can be input manually from the control console. It is also possible to control stagnation pressure, Mach number, and model angle of attack automatically from the same computer used in the data-acquisition system.

Reynolds Number Capability

A plot of the tunnel Reynolds number as a function of Mach number for several stagnation pressures is shown in figure 5. The Reynolds number shown is for a 15.24-cm (6.00-in.) model chord which is the nominal model size for this facility. Although these curves are for a constant stagnation temperature, there is no control over this parameter and it will vary during a tunnel run. With automatic tunnel control, the stagnation pressure can be adjusted to compensate for stagnation-temperature changes, thus providing a constant Reynolds number for the duration of the run.

INSTRUMENTATION

Pressure Instrumentation

At present, the facility is instrumented to obtain static pressure measurements on the airfoil surface and in the wake downstream of the model. A total of 64 channels of commercially available, high-precision, capacitive potentiometer-type pressure transducers are available for this program. A complete description of this type of pressure instrumentation is presented in reference 3. Reference 1 describes the connection of the model pressure leads to these transducers and the electrical connection of transducers to autoranging signal conditioners.

Traversing Survey Probe

Airfoil drag measurements are made by a vertical traversing survey probe system that is located at tunnel station 38.10 cm (15.00 in.) and has a traversing range of z from 25.40 cm (10.00 in.) to -25.40 cm (-10.00 in.) from the tunnel center line. The probe is driven by a closed-loop-control electric drive system and is capable of drive speeds from about 2.54 cm/sec (1.00 in/sec) to about 25.40 cm/sec (10.00 in/sec). The stroke and the speed can be remotely controlled from the operator's panel in the control room. The survey probe position can also be computer controlled where the wake of the model is located and the stroke is adjusted to include only the wake pertinent to the drag calculation. This feature reduces both run time and workload.

The components of the survey system, including the ball screw, guide rods, and position encoder are shown in figure 6. Details of the multitube pitot probe are shown in figure 7. The static pressure downstream of the model used in the drag calculation comes from averaging pressures measured along a vertical row of tunnel sidewall orifices at station 30.48 cm (12.00 in.). The transducers used with the probe are located inside the pressure shell adjacent to the survey system to keep the response time low.

Data-Acquisition System

The data-acquisition system used for the 6- by 28-Inch Transonic Tunnel is shared with other facilities located in the same complex. For the 6- by 28-Inch Transonic Tunnel, this system provides three functions: data acquisition, tunnel control, and preliminary postrun data reduction. A computer, teletype input, and associated electronics are shown in figure 8. The card reader, line printer, and two-axis plotter are shown in figure 9. Details of the system's functions and capabilities are described in reference 1.

Models

A photograph of two typical models tested in the facility is shown in figure 10. Both models are constructed of stainless steel with a span of 15.24 cm (6.00 in.) and are constructed for pressure-distribution tests. The 10.16-cm (4.00-in.) chord model which has tubes laid in the surface and covered with an epoxy-type resin, is held in place on the turntable by highly stressed dowel pins. However, for the high stagnation pressures and high lift coefficients, the preferred type of model construction is as shown on the 15.24-cm (6.00-in.) chord model. In this case, rectangular tangs, machined on the ends of the model, transfer the model aerodynamic loads to the model support system. The tubes have been placed inside the model and a cover plate has been welded in place over the tubes. Both types of model construction have yielded accuracies in airfoil contour to within ± 0.013 mm ($\pm 5.00 \times 10^{-4}$ in.). Typically, orifices have a diameter of 0.34 mm (1.35×10^{-2} in.) and are located in chordwise rows on both surfaces near the model midspan.

TUNNEL CALIBRATION

Flap Calibration

Calibration of the flap involved the determination of the longitudinal Mach number gradients at fixed flap settings as a function of M_{TC} the test-chamber Mach number. The required measurements were concentrated between station 0, the model station, and station 121.92 cm (48.00 in.), where the flap position had the greatest influence on the Mach number gradient. Figures 11 and 12 show the effect on the Mach number gradient for the fully closed and fully open positions, respectively. Most of the calibration data were obtained at a stagnation pressure of 207 kN/m^2 (30 psia), but additional data were also obtained at a stagnation pressure of 517 kN/m^2 (75 psia). Figures 11 and 12 indicate the following effects of the flap on the Mach number gradient:

(1) When the flap is fully closed, the Mach numbers tend to increase in the downstream direction, as if the flow reentering the test section forms an effective throat just downstream of the flap, which ends at station 87.12 cm (34.30 in.). At the higher Mach numbers, near-sonic velocities appear in this region.

(2) When the flap is fully open, the Mach numbers tend to decrease in the downstream direction.

Flap opening positions were varied in 20-percent increments of full travel, and the Mach number range was swept at each increment. Figure 13 shows sidewall Mach number distributions for different values of M_{TC} at the various flap settings. The value of M_{TC} resulting in the lowest Mach number gradient for each flap setting was assigned to that flap setting. The relationship between flap setting and M_{TC} provides the calibration shown in figure 14. The required flap opening for the minimum Mach number gradient increases with increasing free-stream Mach number and becomes fully open at $M_{TC} = 1.00$.

The traversing survey probe has little effect on the sidewall Mach number distribution as is indicated in reference 1. Figure 15 shows data with the probe at $z = 0$ and in the stored position, $z = -29.21$ cm (-11.50 in.). There is a disturbance at the location of the probe, but there is no effect seen at the model station.

Additional sidewall Mach number distributions are presented for $z = -7.62$ cm (-3.00 in.) in figure 16 with the flap at its calibrated position for each M_{TC}. Since these downstream Mach number gradients are comparable to the previous data at $z = 7.62$ cm, these distributions indicate uniform flow along the central part of the test section.

Mach Number Calibration

Originally, it was believed that the presence of the model would have little influence on M_{TC}. Therefore, the local Mach number was measured at the model station, tunnel empty, against the corresponding value of M_{TC} (ref. 4).

8

However, in some instances, the effective free-stream Mach number with the model in place appeared to be lower than the value calibrated with M_{TC}. This effect appeared when the experimental pressure distributions on an airfoil test model were compared with a theoretical pressure distribution on an airfoil of the same shape at the same free-stream Mach number, Reynolds number, and normal-force coefficient. Figure 17 shows a comparison of the experimental and theoretical pressure distributions on the NACA 0012 airfoil at a free-stream Mach number of 0.800 and a lift coefficient of approximately 0.34 at a Reynolds number of 6×10^6. The model had fixed transition at 7.5 percent chord that consisted of a No. 320 carborundum grit strip with the grit particle height determined from reference 5. The theoretical pressure distribution was given by the transonic analysis code of reference 6, which used only a turbulent boundary layer in the computation. For this comparison, the turbulent boundary layer was specified to originate at 7.5 percent chord, the same position as the fixed transition on the test model. The test-model pressure distribution had a slight distortion on the upper surface between 7.5 percent chord and 15 percent chord that was not present in the theoretical pressure distribution. This distortion in the test-model pressure distribution appeared to be a compression followed by an expansion around the transition strip.

Further comparison of the test-model pressure distribution and the theoretical pressure distribution showed a difference in the shock-wave location on the upper surface of the airfoil. Figure 17 indicates that this shock wave began at approximately 45 percent chord for the experimental pressure distribution and at 52 percent chord for the theoretical pressure distribution. In this case, the shock wave on the NACA 0012 airfoil at this normal-force coefficient and Reynolds number travels rearward with increasing free-stream Mach number. The previously mentioned difference in shock-wave locations between the experimental and theoretical pressure distributions indicated that the free-stream Mach number used with the experimental data might be slightly high.

Two probable causes for error in tunnel free-stream Mach number were wind-tunnel blockage and the Mach number calibration method. Although both of these problems were addressed, only the error caused by the free-stream Mach number calibration is presented in this report because it was more easily assessed than the tunnel blockage.

A more accurate determination of stream Mach number at the model station appeared possible by using a local test-section Mach number upstream of the model station in place of M_{TC} in the calibration procedure. This local test-section Mach number was determined from the tunnel sidewall pressure located 66.04 cm (26.00 in.) upstream of the model station and 7.62 cm (3.00 in.) above the tunnel center line. The tunnel-empty model-station Mach number was then correlated with this upstream Mach number M_{US}. The free-stream calibrated Mach number obtained with this procedure was designated M_∞'. Figure 18 shows M_{US} plotted against M_∞'. For several airfoil tests, both M_{TC} and M_{US} have been used to determine free-stream Mach numbers. The free-stream Mach numbers determined by using M_{US} have been 0.004 to 0.012 lower than those determined by using M_{TC}.

Some concern arose over the model upwash at the upstream station used for M_{US} causing a vertical pressure gradient as observed in the Langley Low Turbulence Pressure Tunnel. The local pressures along a vertical row of sidewall orifices at the upstream station were measured with the tunnel empty and with a model installed. Figure 19 shows the resulting Mach numbers from these pressures at various M_∞' where the model used (NACA 65_1-213, a = 0.5 airfoil) was larger than the standard size (NACA 0012 airfoil) usually tested (20.32 cm (8.00 in.) compared with 15.24 cm (6.00 in.)). The model appeared to have only small effects along this vertical line through the upstream station, resulting in no appreciable vertical pressure gradient, and thus simplifying the calibration process.

After the uniformity of the vertical Mach number distribution was established, the theoretical and test-model pressure distributions on the NACA 0012 airfoil were compared again in a manner similar to that described for figure 17. Figure 20 shows a comparison of the same model pressure distribution shown in figure 17, but with the free-stream Mach number determined from M_{US} instead of M_{TC}. Here, the free-stream Mach number M_∞' is 0.794, and using this free-stream Mach number in the transonic analysis code results in a theoretical pressure distribution that matches the model pressure distribution significantly closer than the comparison in figure 17. The shock-wave position for the theoretical pressure distribution now begins at 48 percent chord, which is much closer to the model shock-wave position than that shown in figure 17. The theoretical pressure distribution still differs from the model pressure distribution in the region between 7.5 percent chord and 15 percent chord in both upper and lower surfaces because of the local distortion caused by the transition strip located at 7.5 percent chord on the model.

Since the free-stream dynamic pressure is reduced when calculated from M_∞' instead of M_∞, higher absolute values of normal-force and pitching-moment coefficients are achieved. The drag coefficient is also increased because of the increase in point drag coefficient measured in the model wake, as indicated in reference 7. Figure 21 shows the differences in the normal-force, pitching-moment, and drag data for a 20.32 cm (8.00 in.) chord model (NACA 65_1-213, a = 0.5 airfoil), which is larger than the normal size model tested (15.24 cm (6.00 in.)). This larger than normal model provides an upper bound on the differences between M_∞ and M_∞'.

CONCLUSIONS

The Langley 6- by 28-Inch Transonic Tunnel has been calibrated for controllable reentry flaps and redesigned top and bottom slotted walls. The following conclusions are based on the performance of the new test-section configuration:

1. The new slotted walls and the controllable reentry flaps result in acceptable tunnel-empty Mach number distributions in the test section.

2. The position of the controllable reentry flaps is independent of tunnel stagnation pressure and varies only with tunnel Mach number.

3. The free-stream Mach number can be more accurately determined from the pressure in the test section at 66.04 cm (26.00 in.) upstream of the model station than from the plenum pressure. The model appears to have no significant influence on the vertical Mach number distribution at 66.04 cm (26.00 in.) upstream of the model station.

Langley Research Center
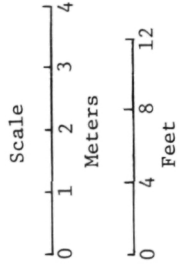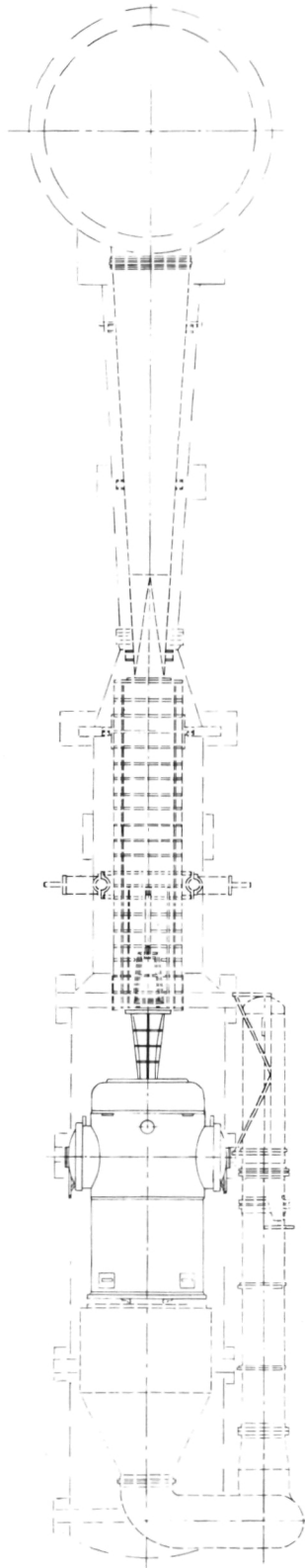National Aeronautics and Space Administration
Hampton, VA 23665
March 20, 1981

REFERENCES

1. Ladson, Charles L.: Description and Calibration of the Langley 6- by 28-Inch Transonic Tunnel. NASA TN D-8070, 1975.

2. Barnwell, Richard W.: Design and Performance Evaluation of Slotted Walls for Two-Dimensional Wind Tunnels. NASA TM-78648, 1978.

3. Bynum, D. S.; Ledford, R. L.; and Smotherman, W. E.: Wind Tunnel Pressure Measuring Techniques. AGARD-AG-145-70, Dec. 1970.

4. Squire, L. C.; and Stanbrook, A.: The Influence of a Model on Plenum Chamber Indication of Mach Number in a Slotted Wall Wind Tunnel. C.P. No. 395, British A.R.C., 1958.

5. Braslow, Albert L.; and Knox, Eugene C.: Simplified Method for Determination of Critical Height of Distributed Roughness Particles for Boundary-Layer Transition at Mach Numbers From 0 to 5. NACA TN 4363, 1958.

6. Bauer, Frances; Garabedian, Paul; Korn, David; and Jameson, Antony: Supercritical Wing Sections II. Volume 108 of Lecture Notes in Economics and Mathematical Systems, Springer-Verlag, 1975.

7. Baals, Donald D.; and Mourhess, Mary J.: Numerical Evaluation of the Wake-Survey Equations for Subsonic Flow Including the Effect of Energy Addition. NACA WR L-5, 1945. (Formerly NACA ARR L5H27.)
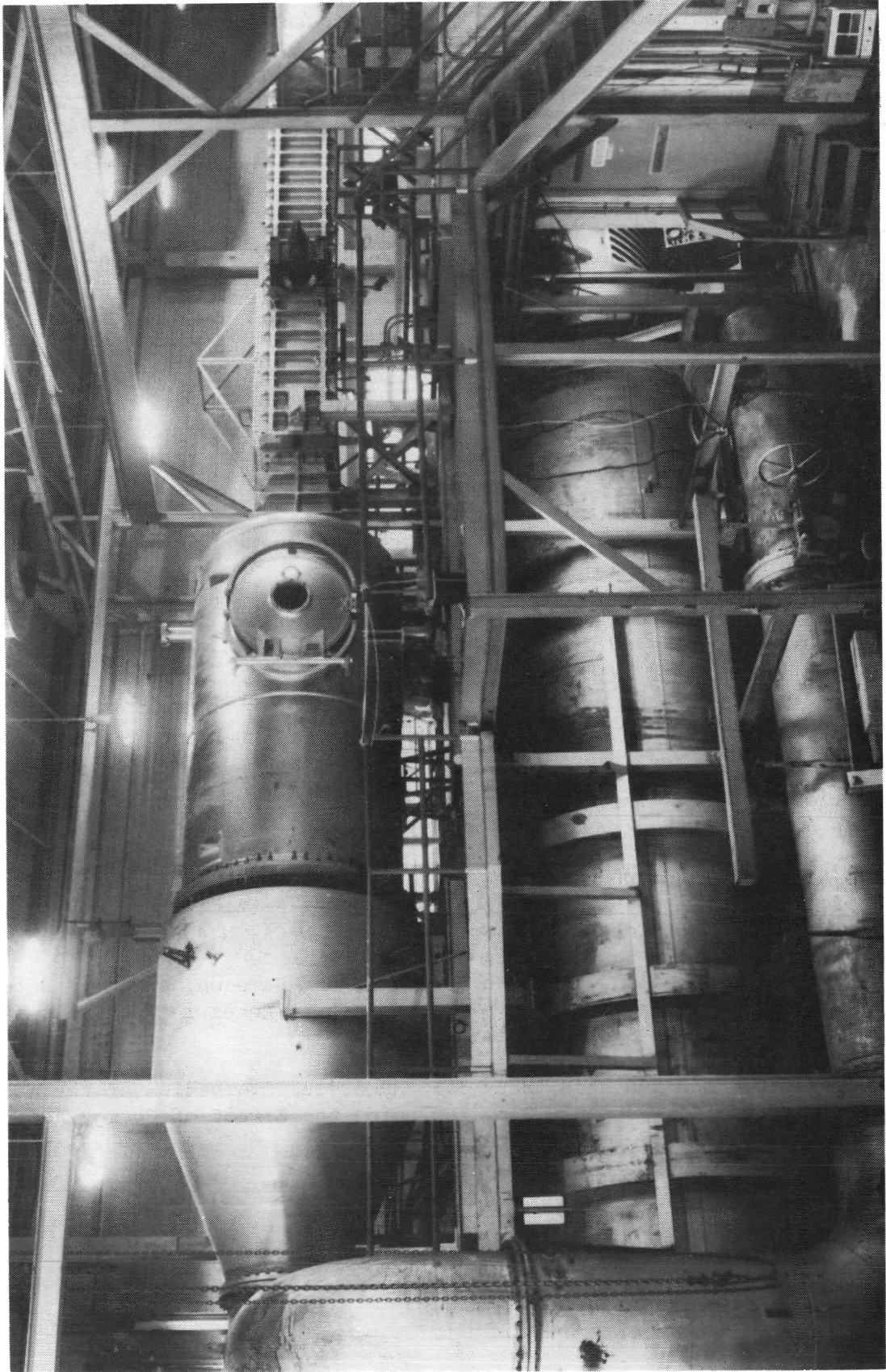
L-75-224

Figure 1.- Overall view of Langley 6- by 28-Inch Transonic Tunnel during assembly.

Planform

Scale

0 1 2 3 4
Meters

0 4 8 12
Feet

6- by 28-Inch Transonic Tunnel

New test section

Settling chamber

6- by 28-Inch Transonic Tunnel

26-Inch Transonic Blowdown Tunnel

Gate valve

Stack

Isolation valve
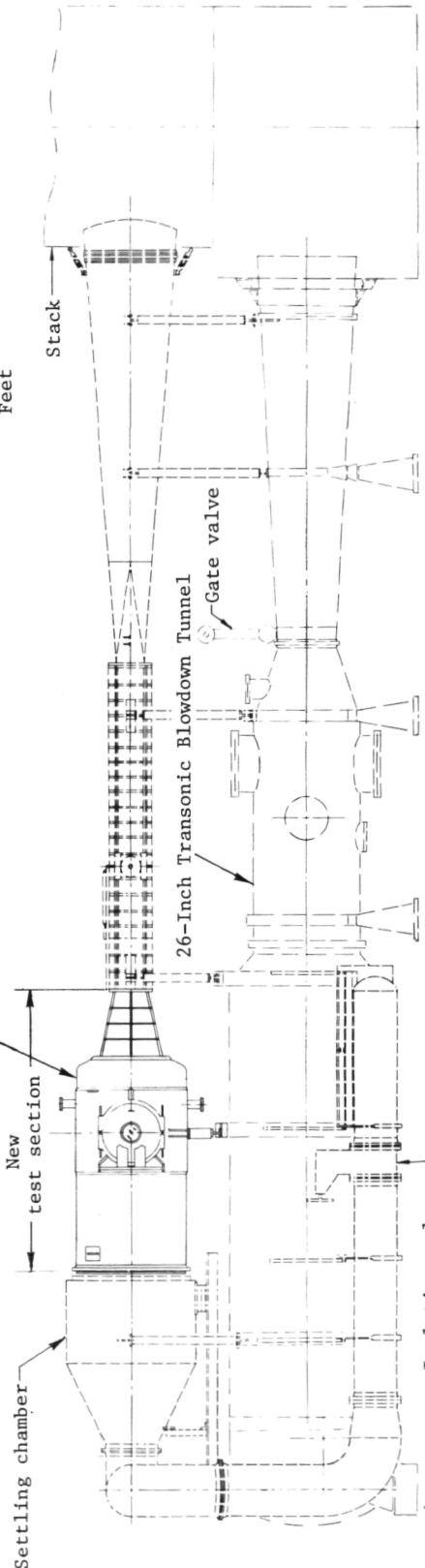
Elevation

Figure 2.- Assembly drawing of 6- by 28-Inch Transonic Tunnel.
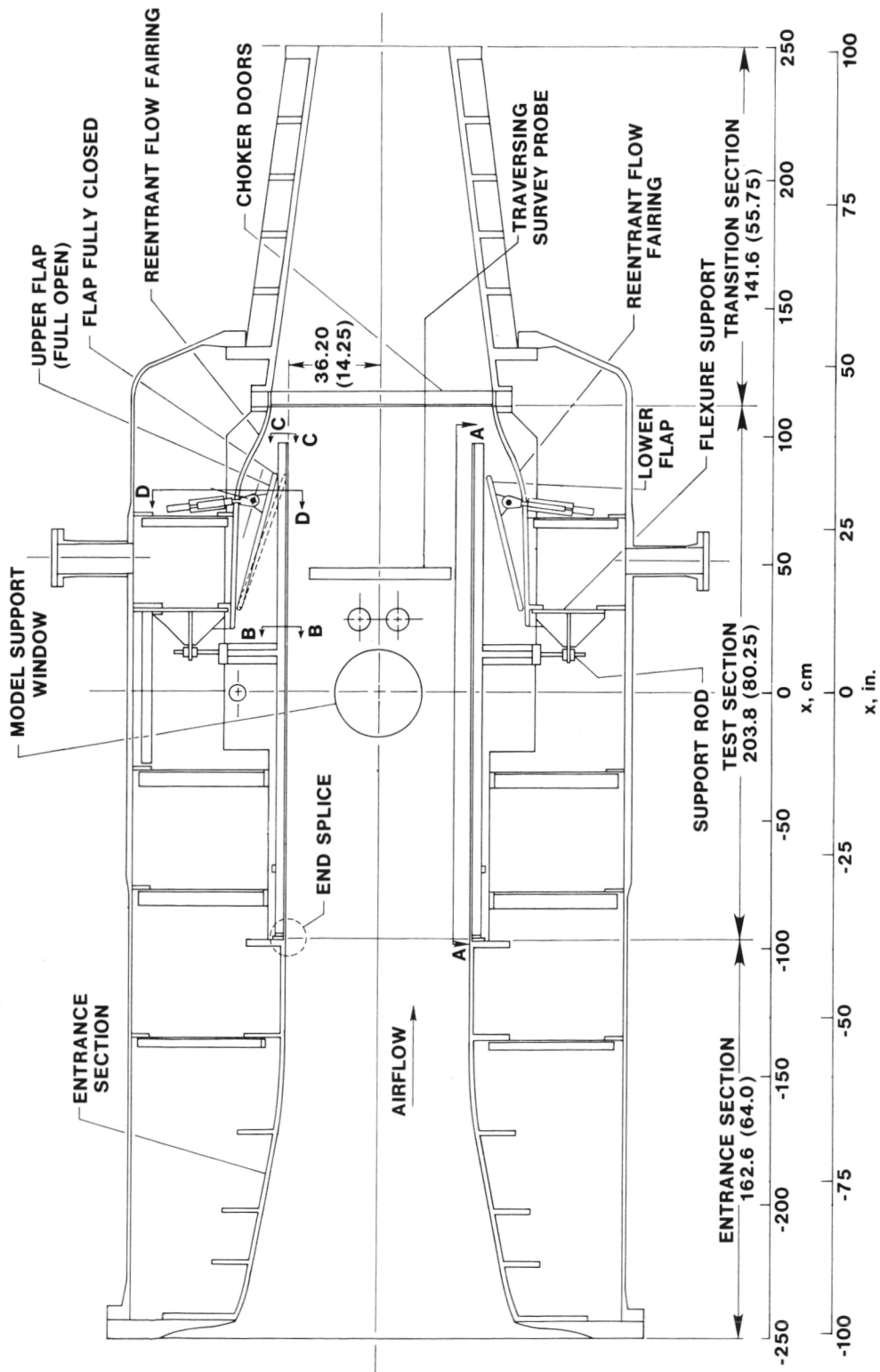
(a) General arrangement.

Figure 3.— Cross-section drawing of side view of Langley 6- by 28-Inch Transonic Tunnel. All dimensions are in centimeters (inches).

14

COUNTERSUNK SCREWS

2 HALF SLOTS

MODEL STATION

3 SLOTS

.236
(.093)

.472
(.186)

153.7 (60.500)

45.7 (18.00)

SLOTS START

8.89
(3.50)

CONSTANT SLOT GAP
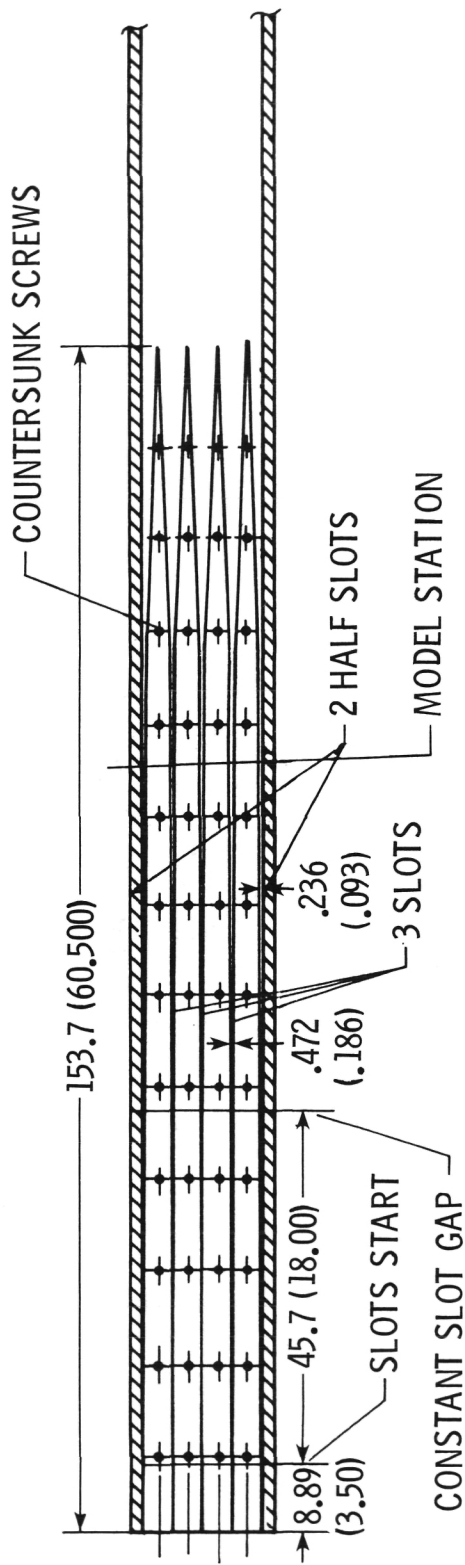
ORIGINAL SLOTTED WALLS: 12.5 PERCENT OPENNESS RATIO

COUNTERSUNK SCREWS

PIN SUPPORT

MODEL STATION

2 HALF
SLOTS

.381 (.150)

CONSTANT
SLOT GAP

.381
(.150)

194.3 (76.5)

SLOTS
START HERE

25.4 (10.00)

5.08
(2.00)
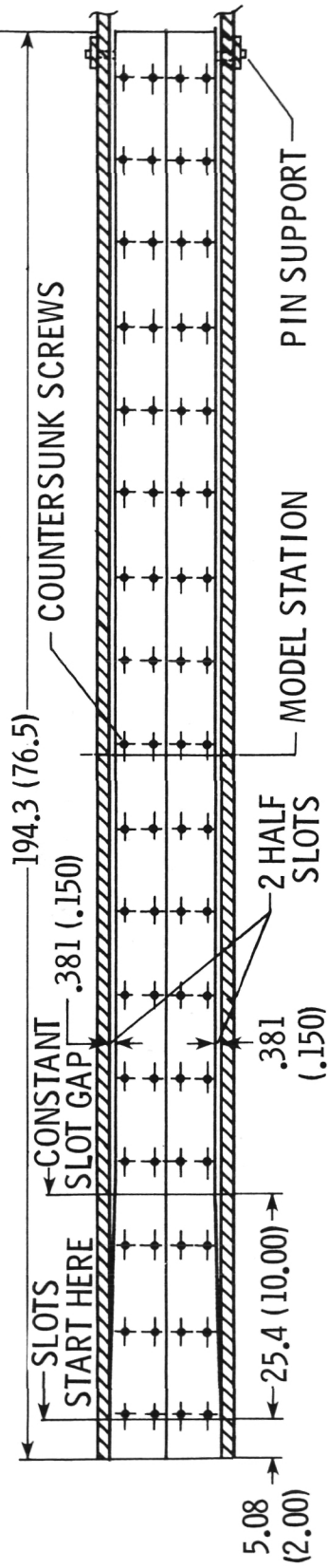
PRESENT SLOTTED WALLS: 5.0 PERCENT OPENNESS RATIO

(b) Section A-A. Slotted top and bottom walls in test section of Langley
6- by 28-Inch Transonic Tunnel.

Figure 3.- Continued.

15
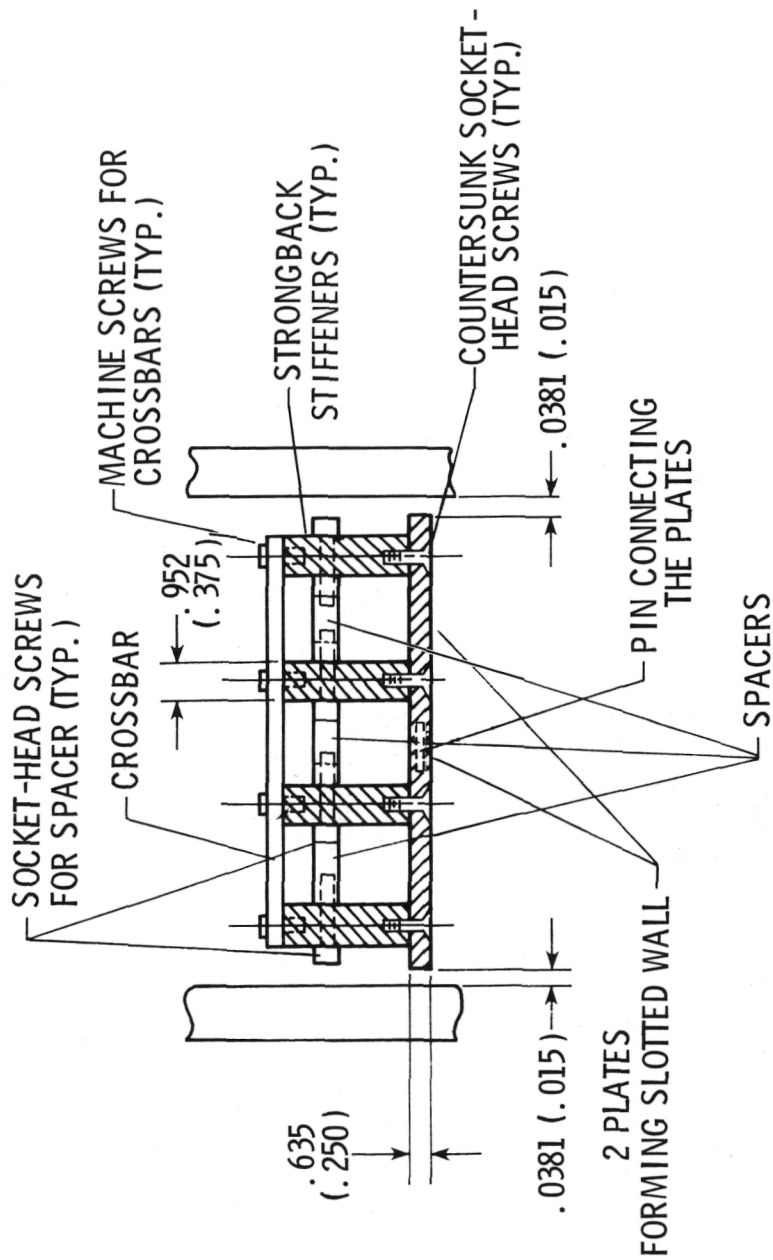
(c) Section B-B. Details of slotted-wall assembly.

Figure 3.- Continued.

Entrance cone

Socket-head screw

Strongback stiffener

End splice plate

End splice

Pin

Set screw
(typ.)

Strongback stiffener (typ.)

Test section

15.24 (6.00)
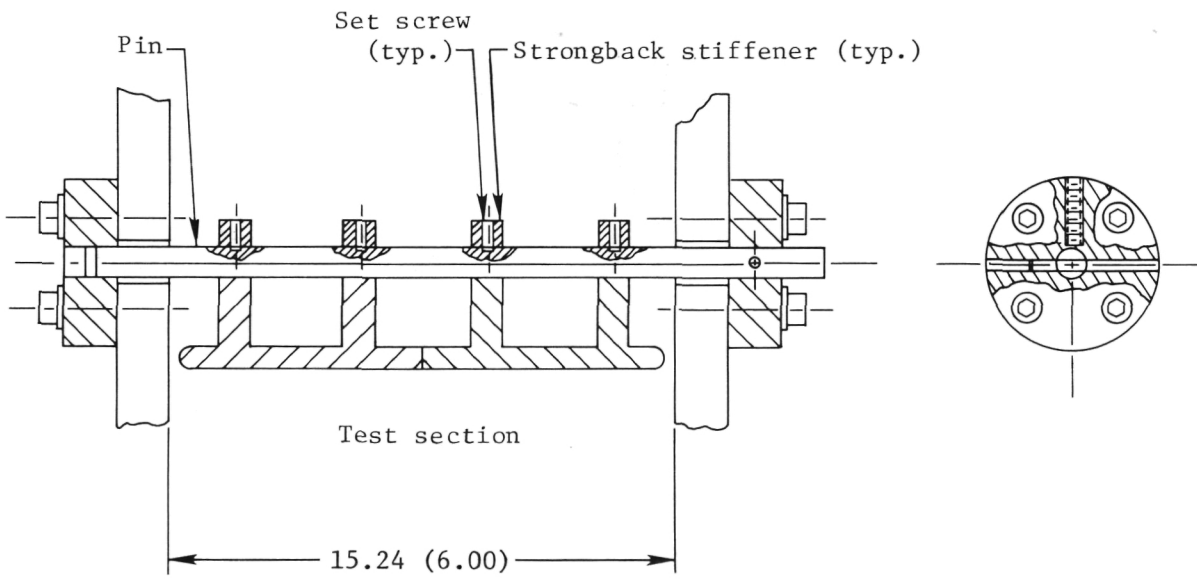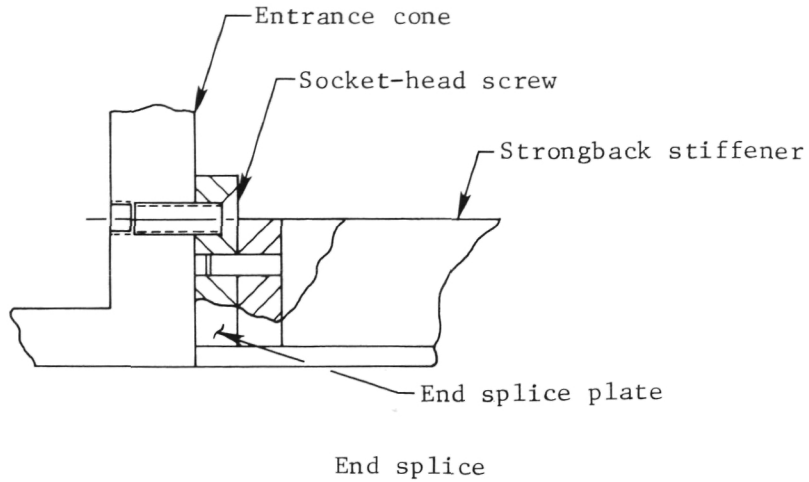
Section C-C. Pin support

(d) Supports for slotted walls in Langley 6- by 28-Inch Transonic Tunnel.

Figure 3.- Continued.

17
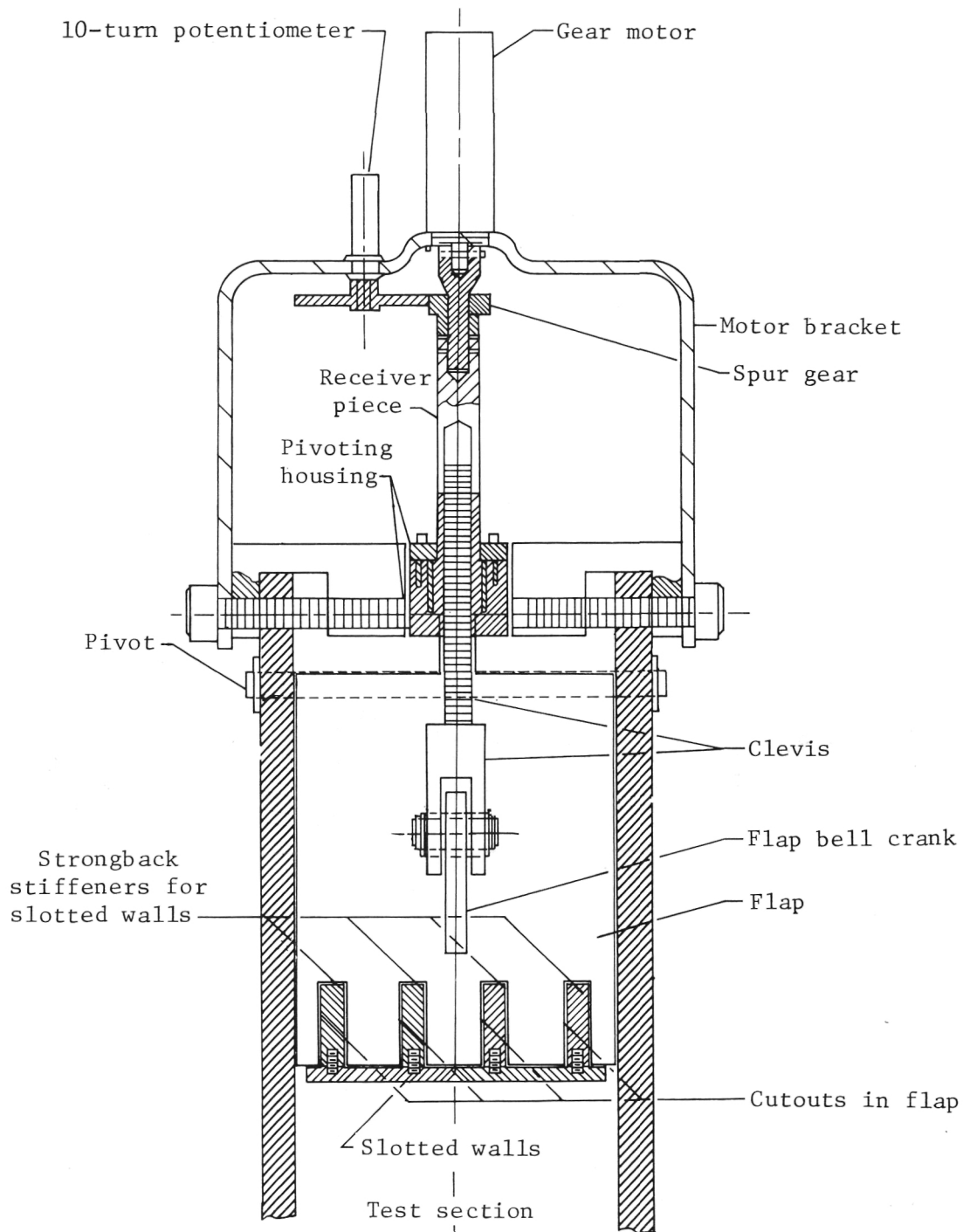
(e) Section D-D.   Details of flap assembly and actuating mechanism.

Figure 3.- Concluded.
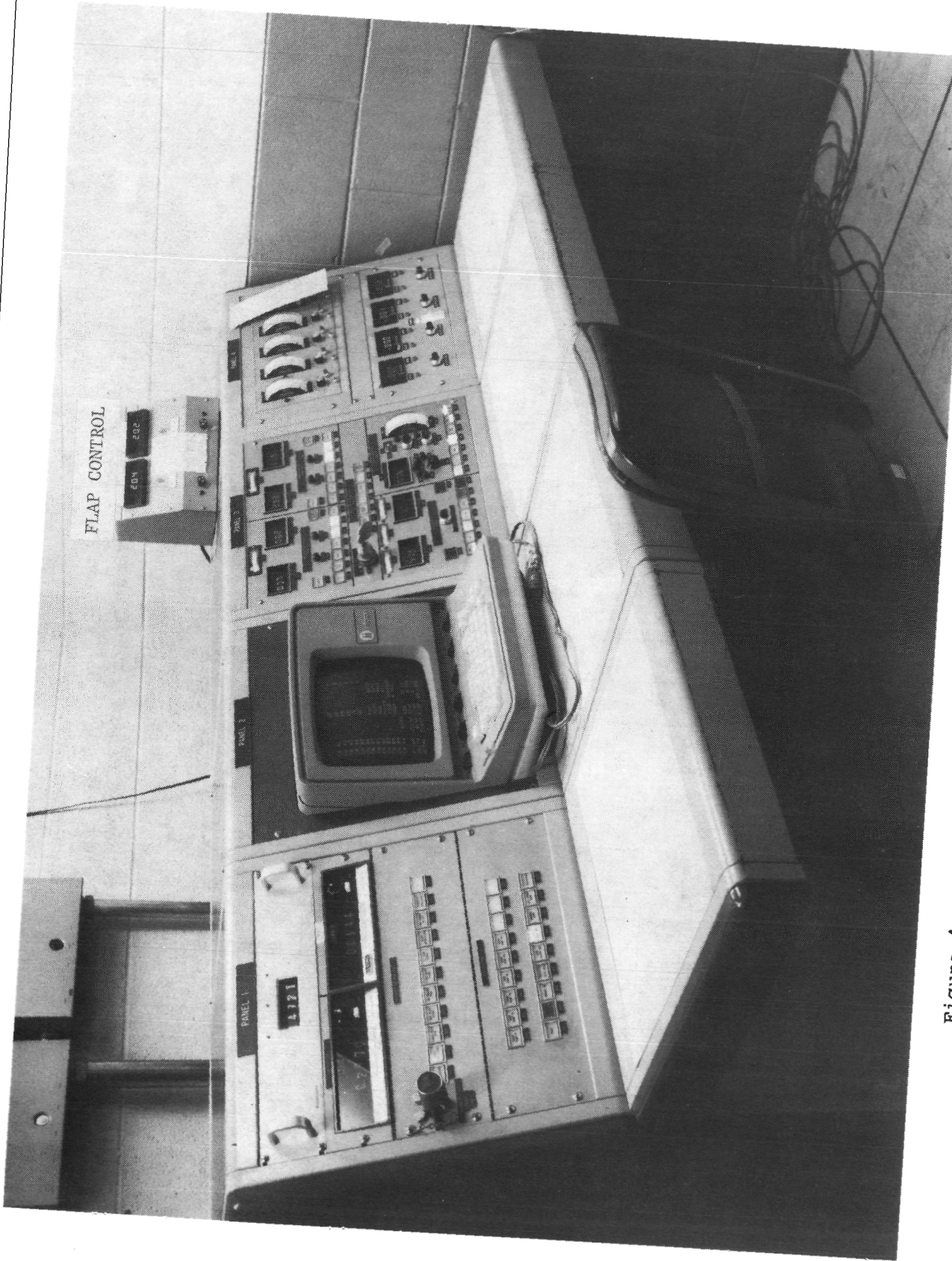
Figure 4.- Tunnel operator's control console with flap control.

L-79-2116.1

19
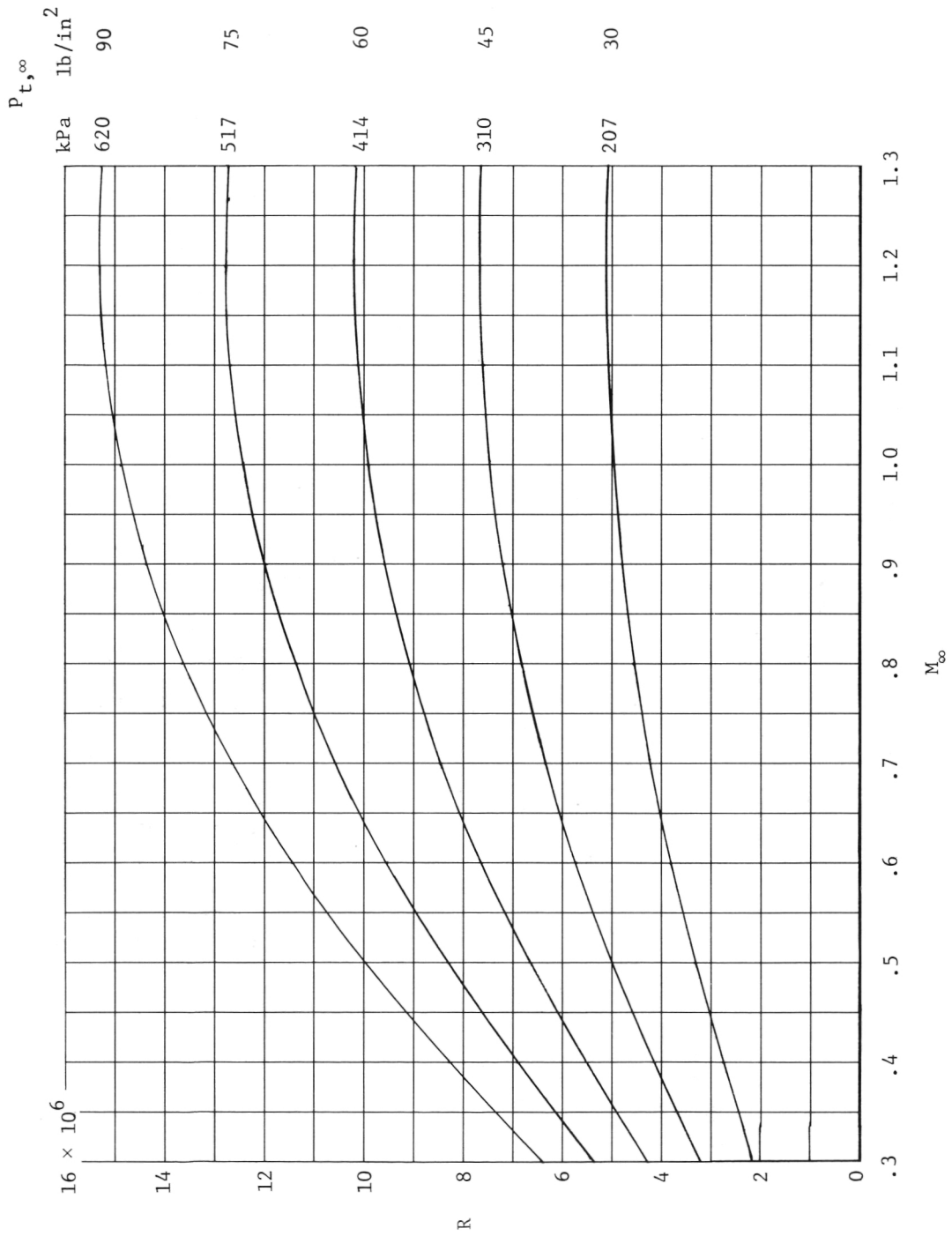
Figure 5.- Reynolds number capability of Langley 6- by 28-Inch Transonic Tunnel. T_t = 283 K (510° R); c = 15.24 cm (6.00 in.).
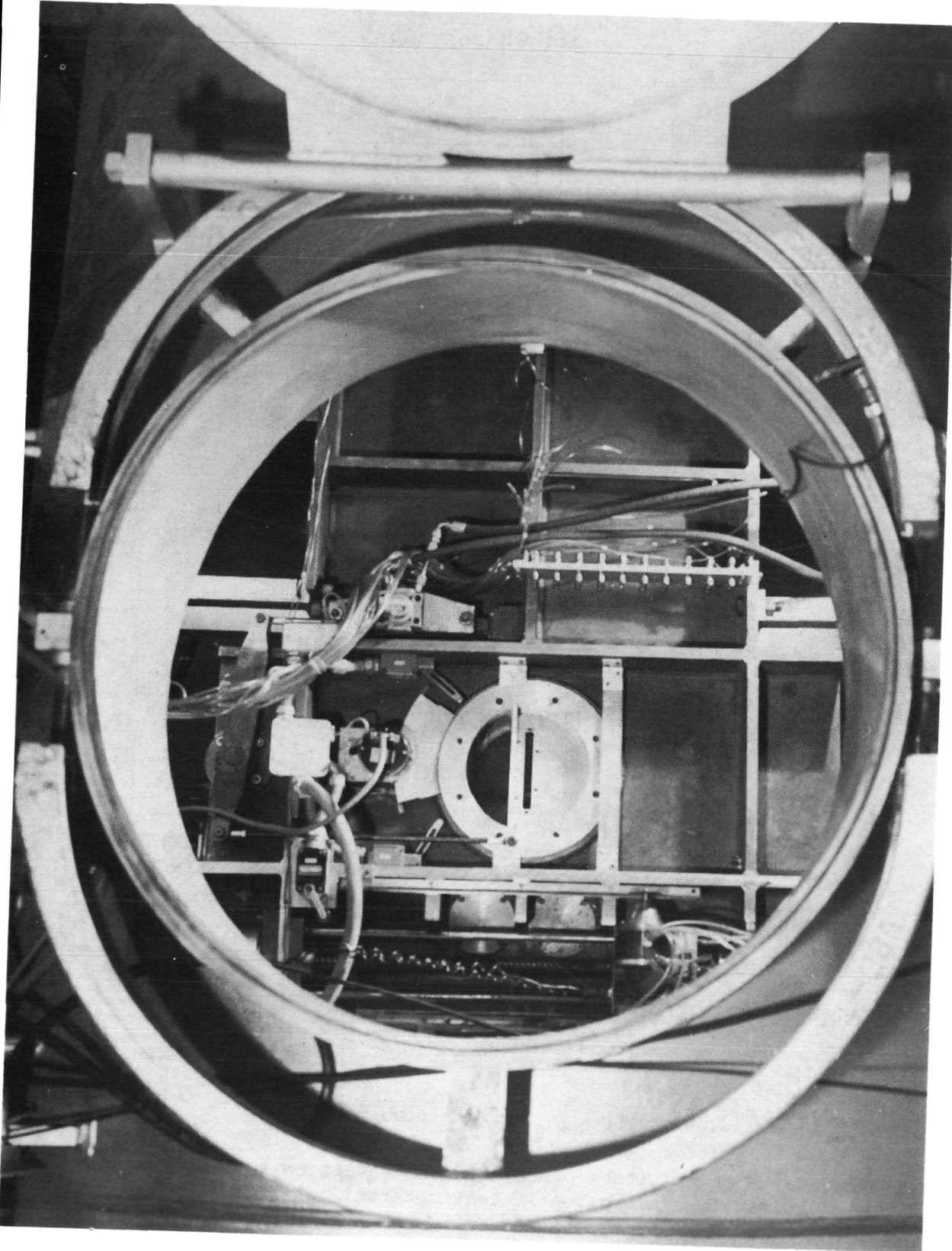
Figure 6.- Interior view of tunnel showing test-section area, model support window, and traversing survey probe mechanism.

L-75-229

Station 38.1 (15.0)

Airflow

9.40 (3.70)

A ↓   ↓ A

℄

5.08 (2.00)

15.24 (6.00)

Inside diameter, 0.102 (0.040)

2.54 (1.00)   5.08 (2.00)
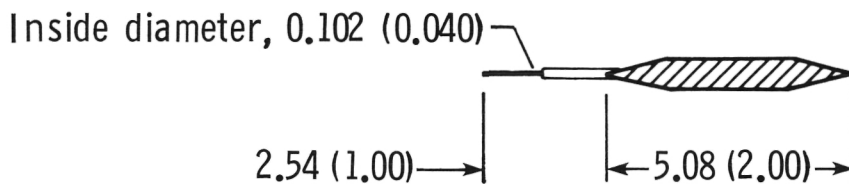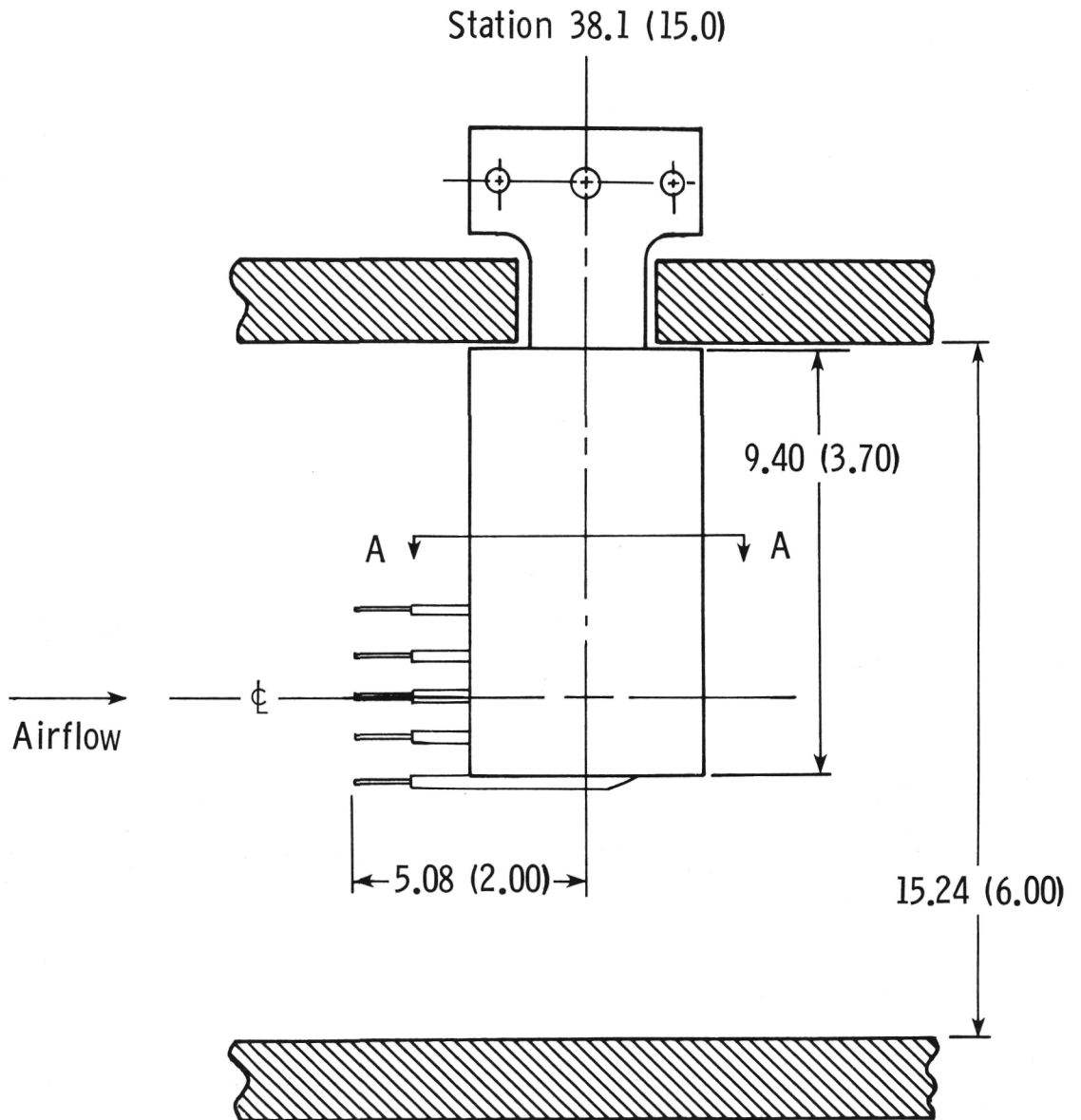
Figure 7.- Details of multitube probe used on traversing survey mechanism.
Dimensions are given in centimeters (inches).
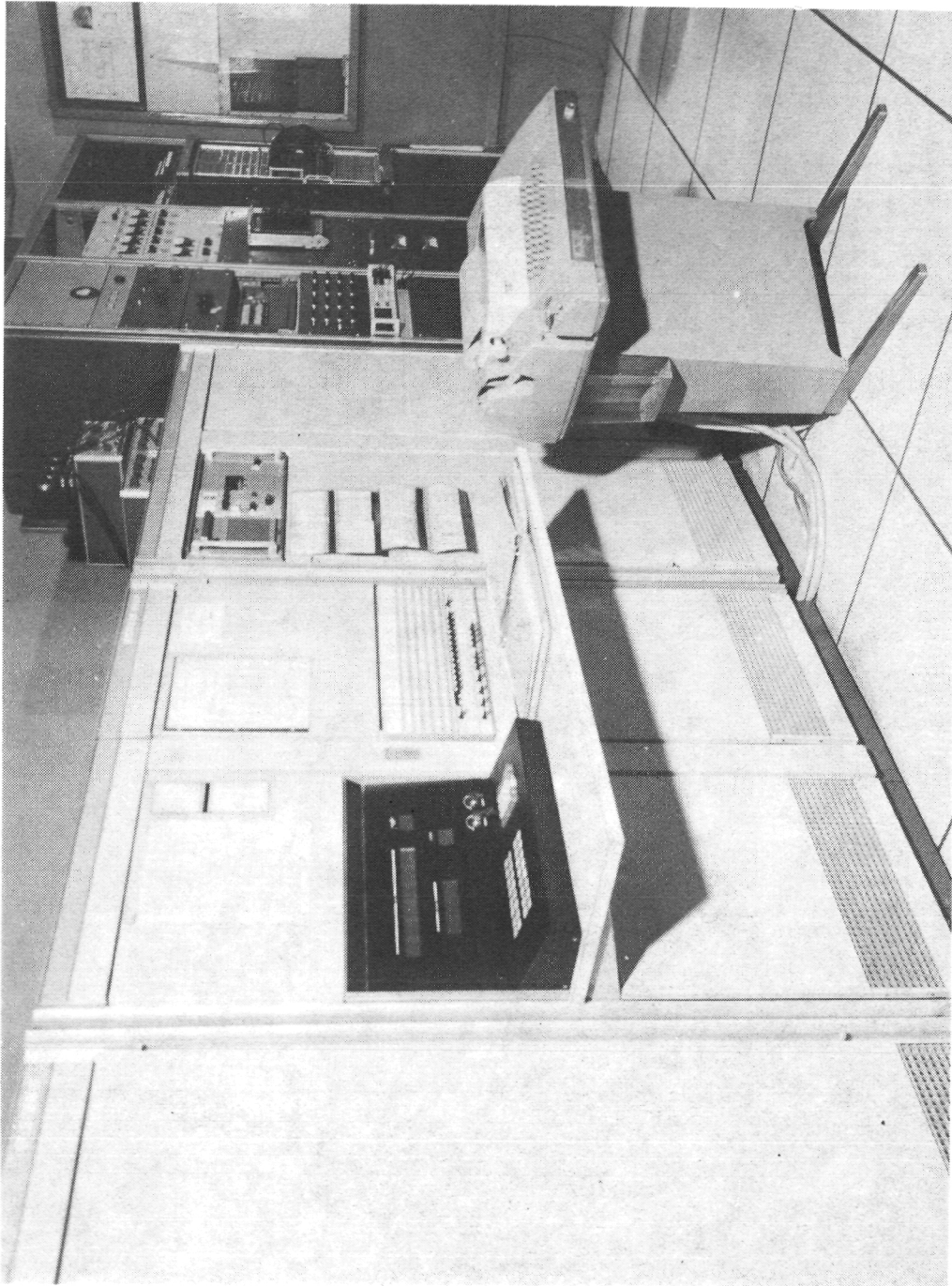
Figure 8.- Overall view of data-acquisition system showing computer and teletype input.

L-75-231

23
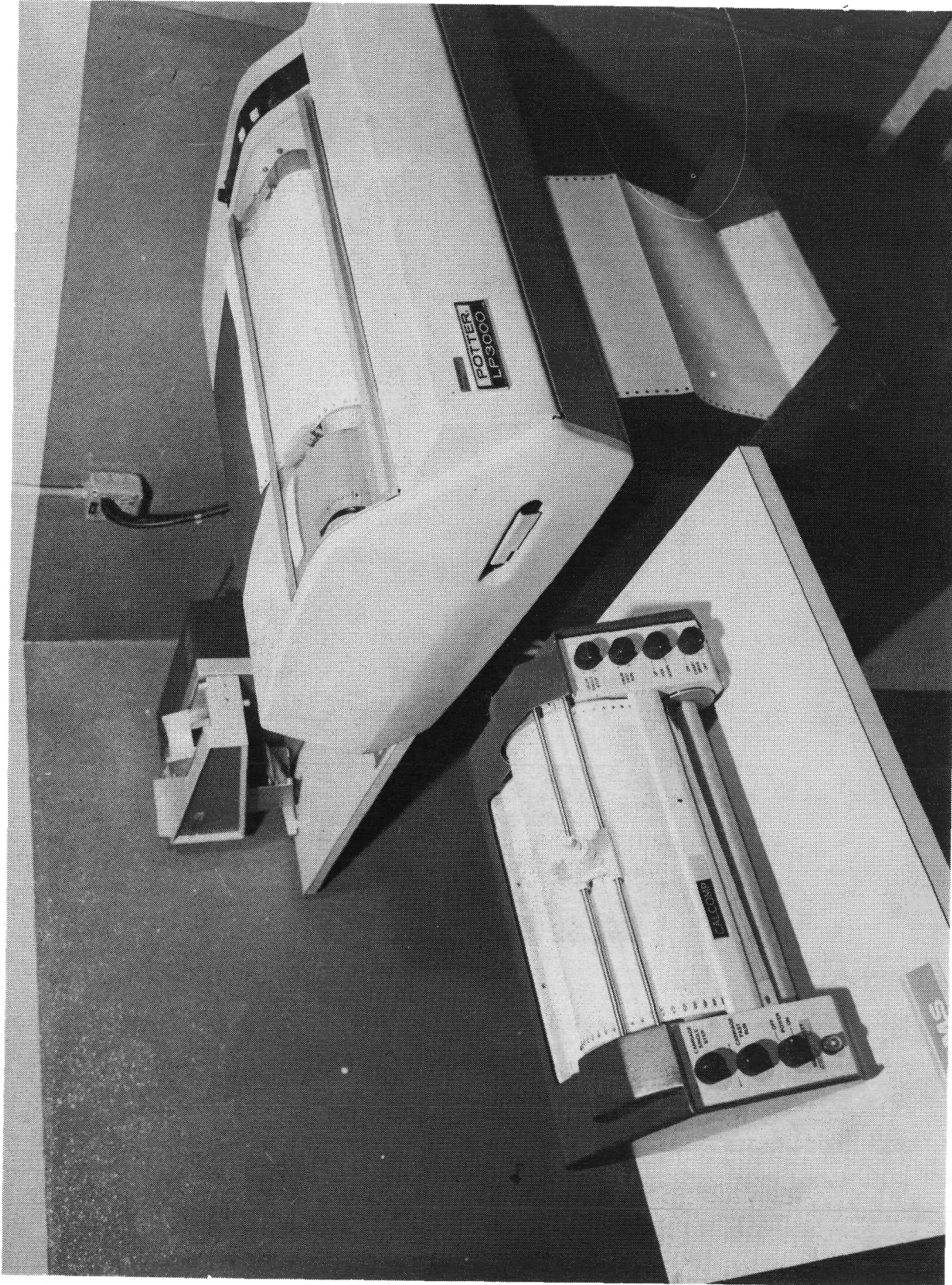
Figure 9.– Card reader, plotter, and line printer used with data-acquision system.
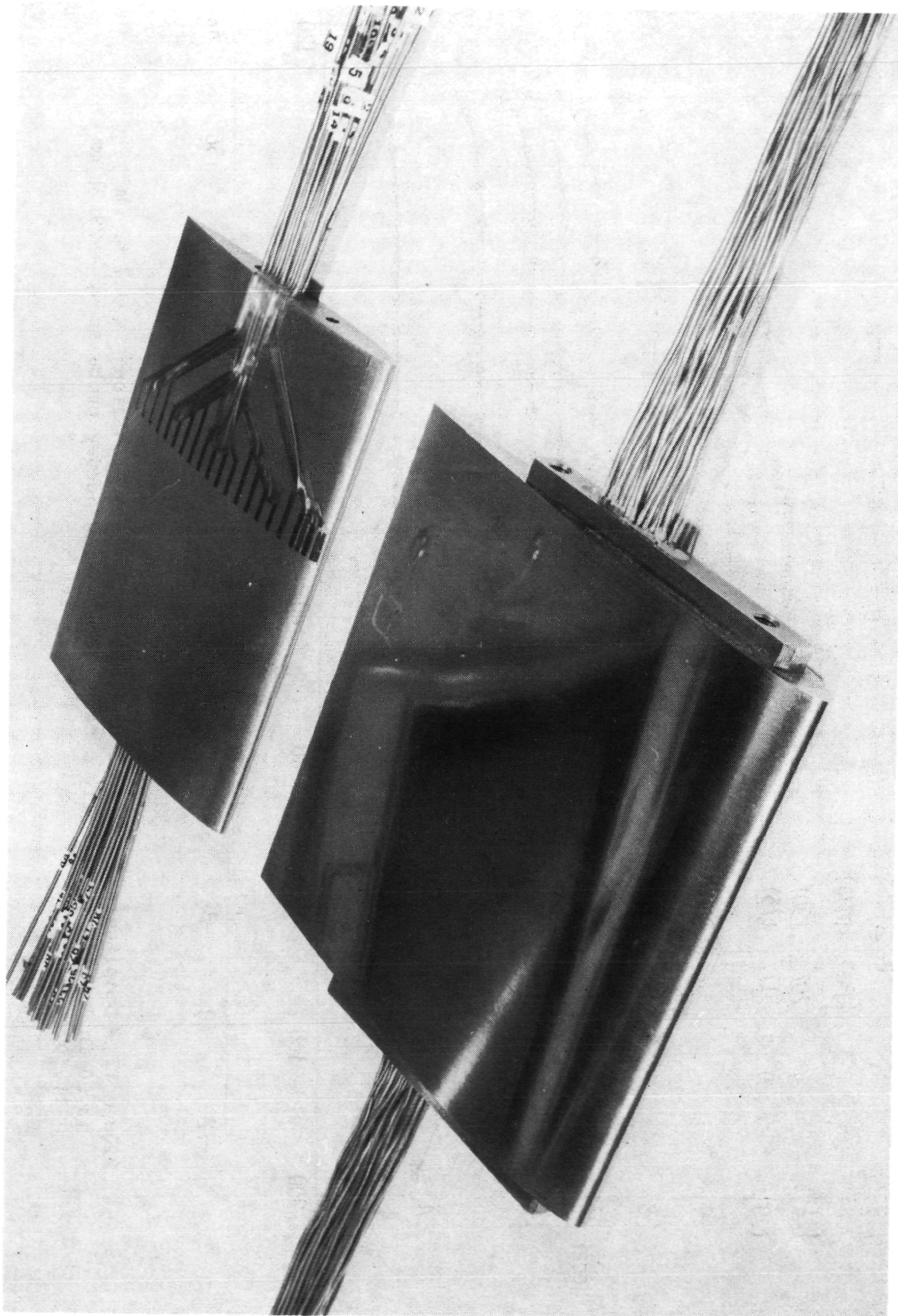
L–75–233

Figure 10.- Typical airfoil models instrumented for pressure tests. 15.24-cm (6.00-in.) chord model in foreground and 10.16-cm (4.00-in.) chord model in background.

L-75-234
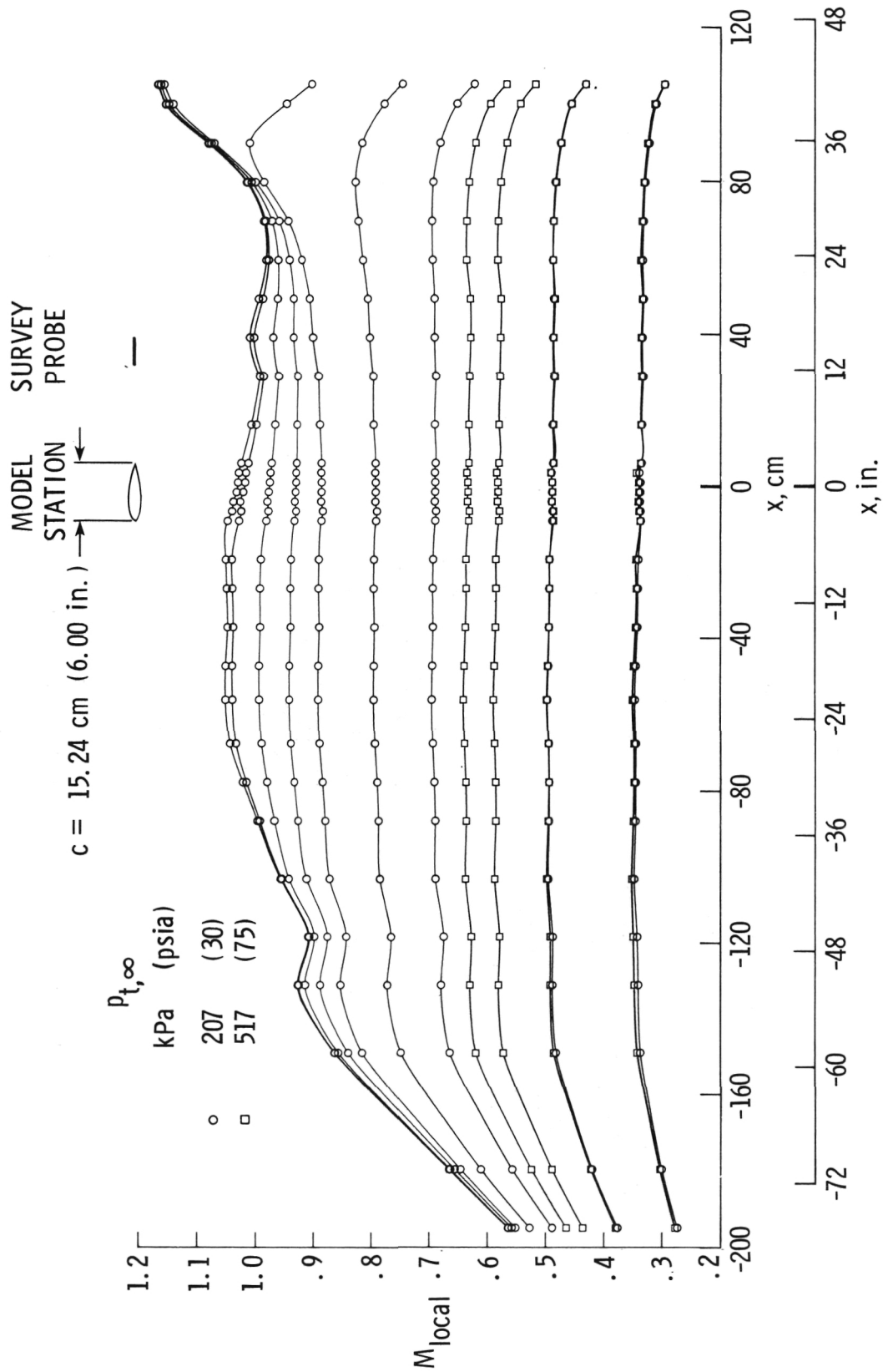
Figure 11.- Longitudinal sidewall Mach number distribution along z = 7.62 cm (3.00 in.) with flaps fully closed. Traversing survey probe at z = 29.21 cm (-11.50 in.).
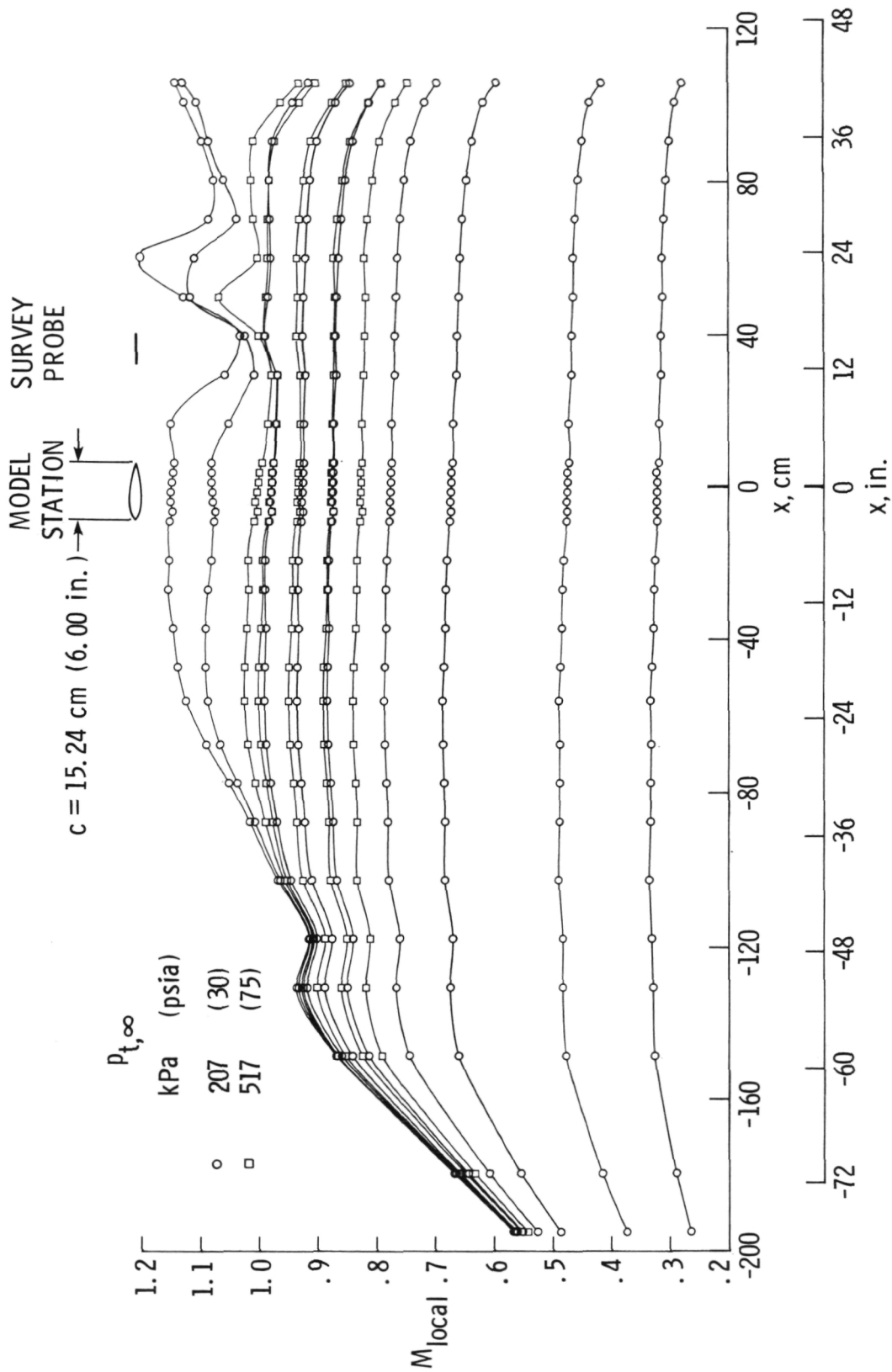
Figure 12.- Longitudinal sidewall Mach number distribution along z = 7.62 cm (3.00 in.) with the flap fully open. Traversing survey probe at z = -29.21 cm (-11.50 in.).
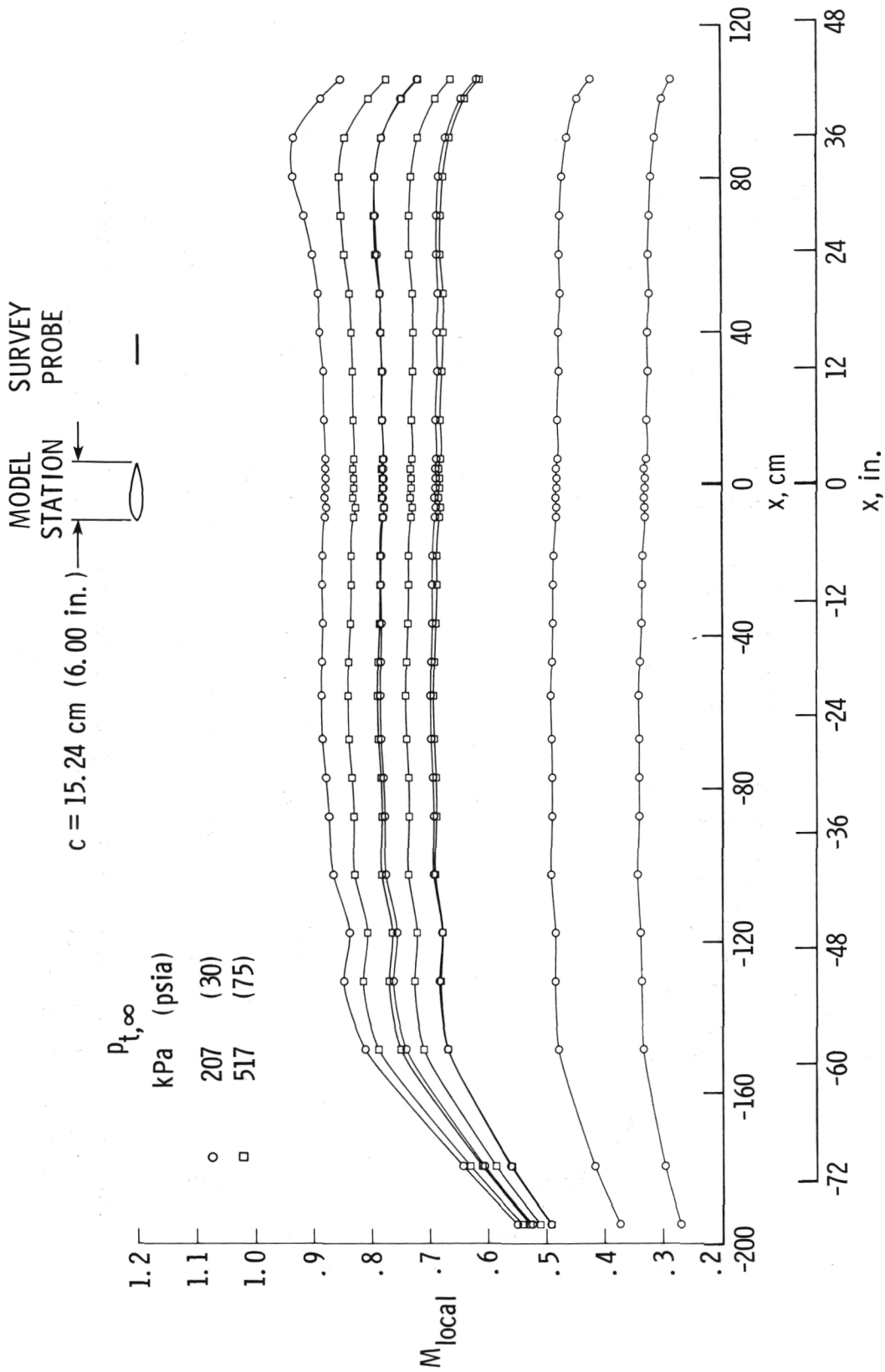
(a) Flaps 20 percent open.

Figure 13.- Longitudinal sidewall Mach number distribution along z = 7.62 cm (3.00 in.). Traversing survey probe at z = -29.21 cm (-11.50 in.).
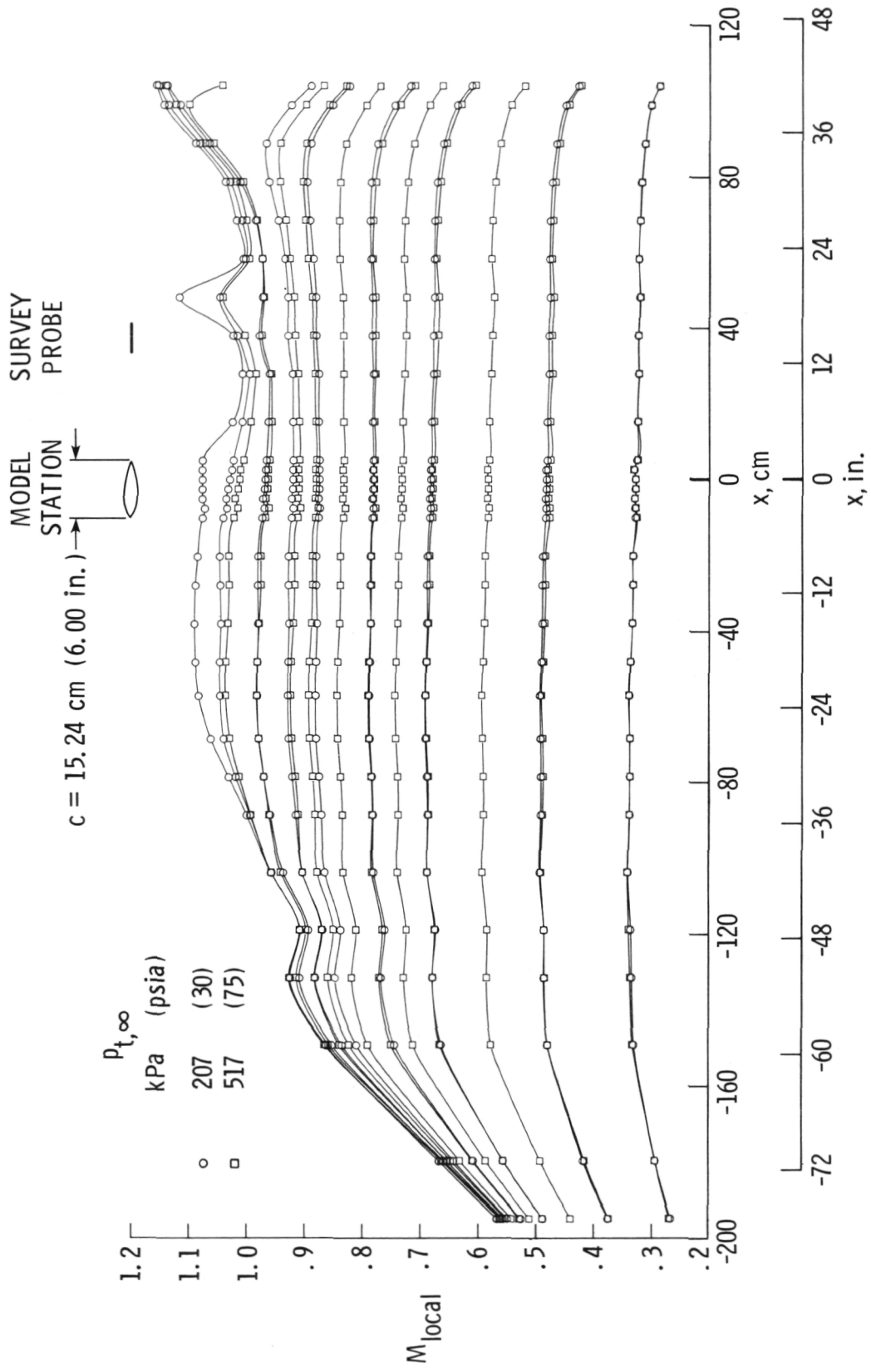
(b) Flaps 40 percent open.

Figure 13.- Continued.
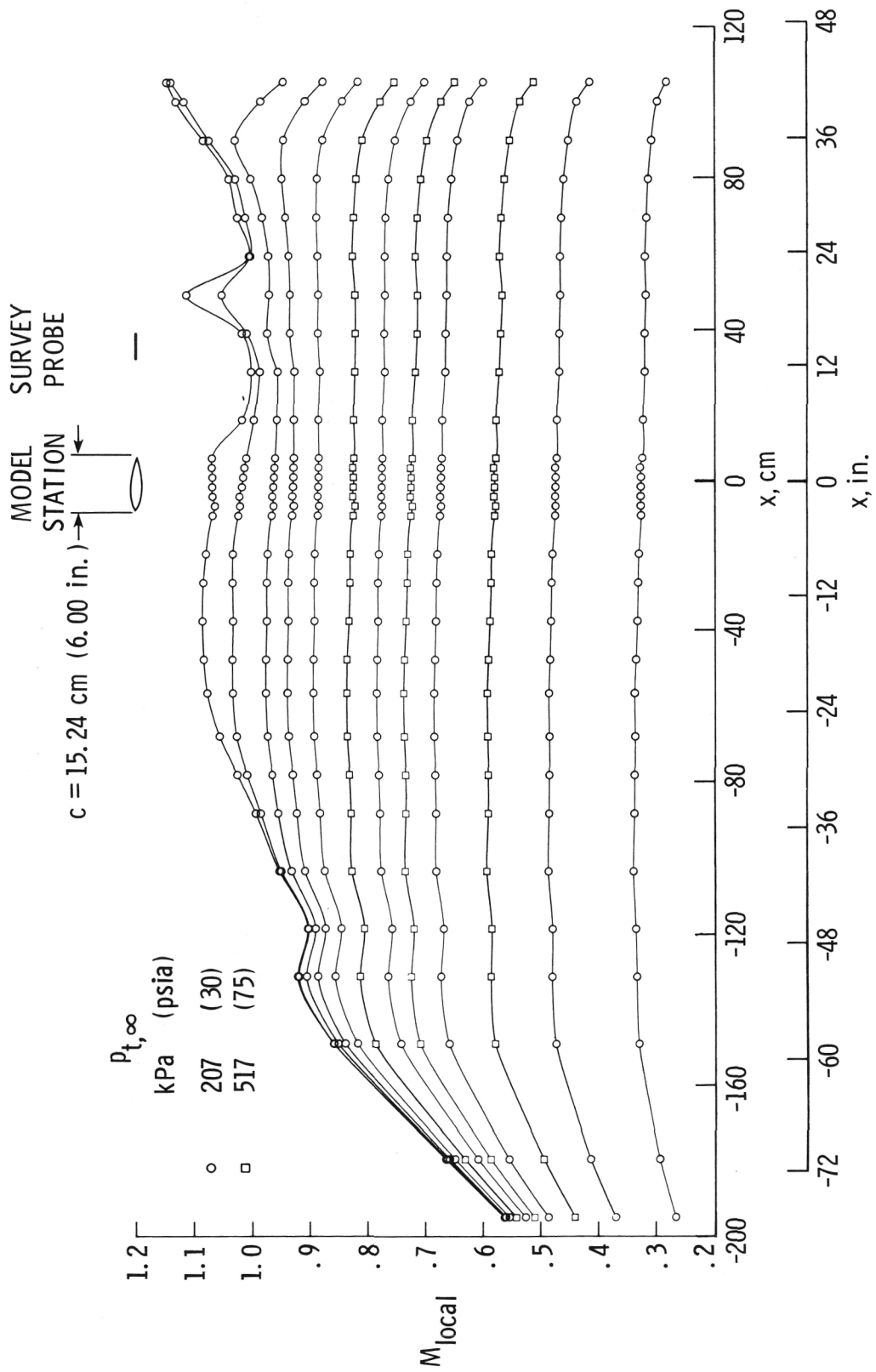
(c) Flaps 60 percent open.

Figure 13.- Continued.
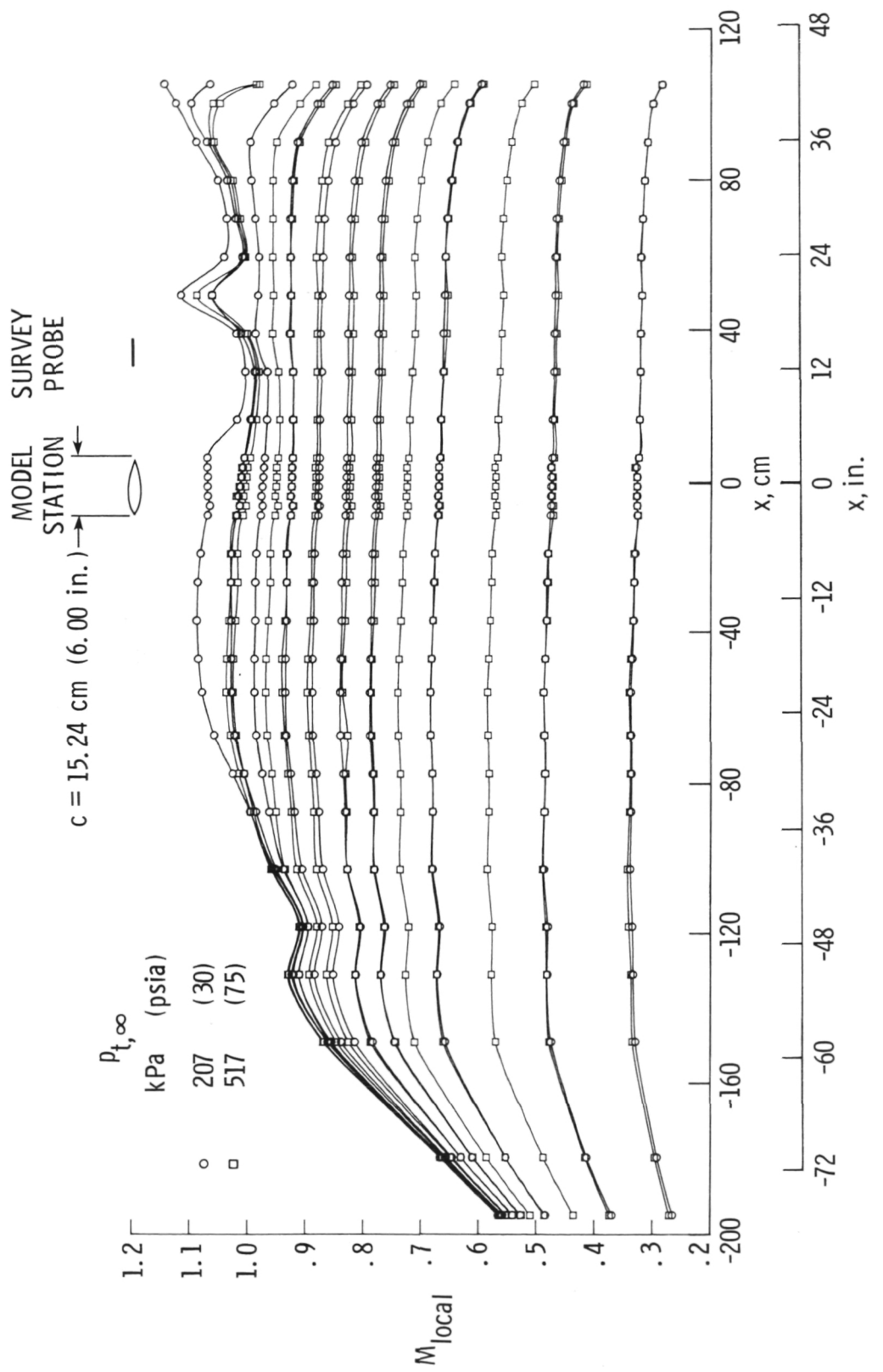
(d) Flaps 80 percent open.

Figure 13.- Concluded.

31
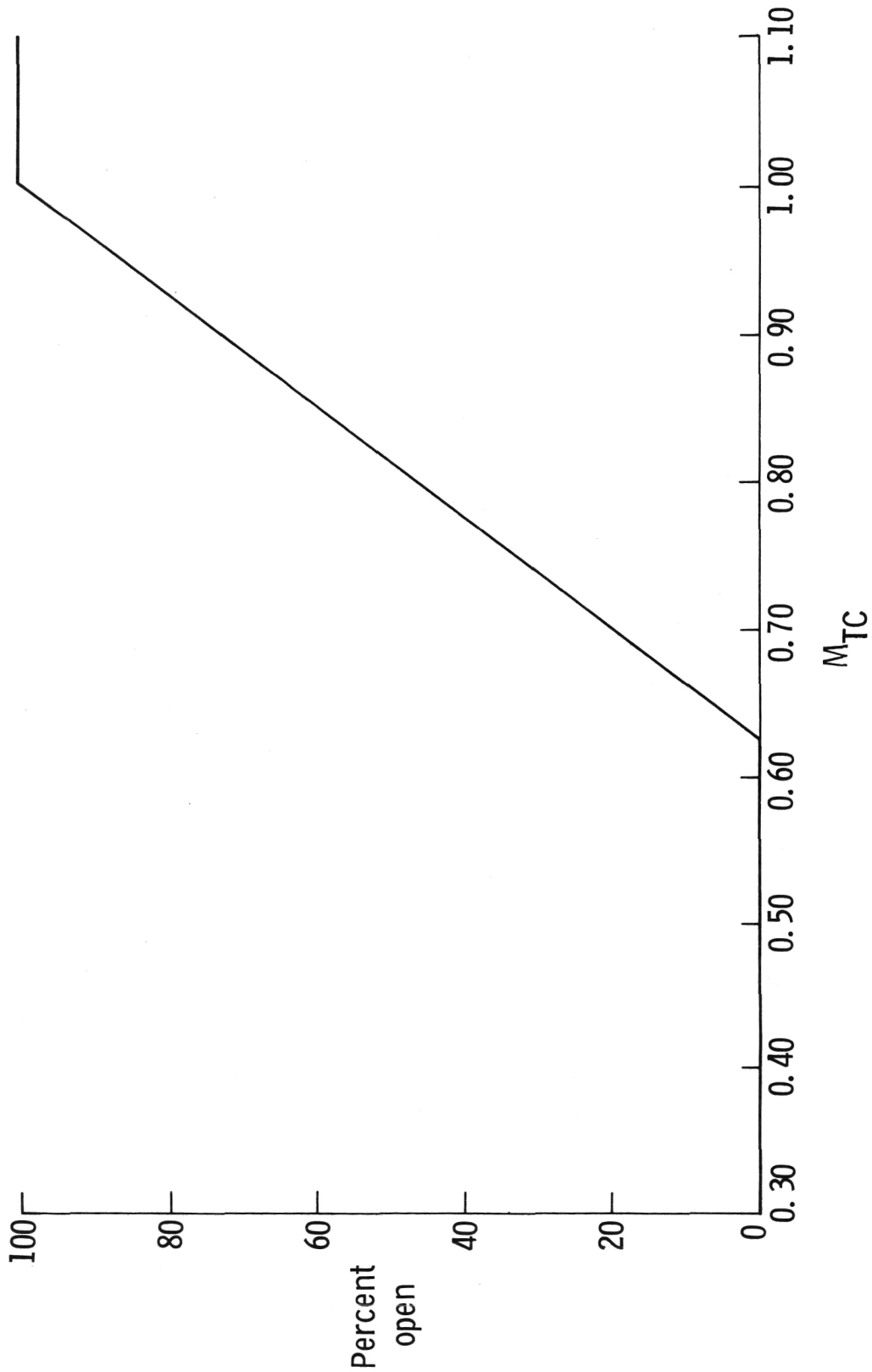
Figure 14.- Variation of flap openness with M_{TC}.
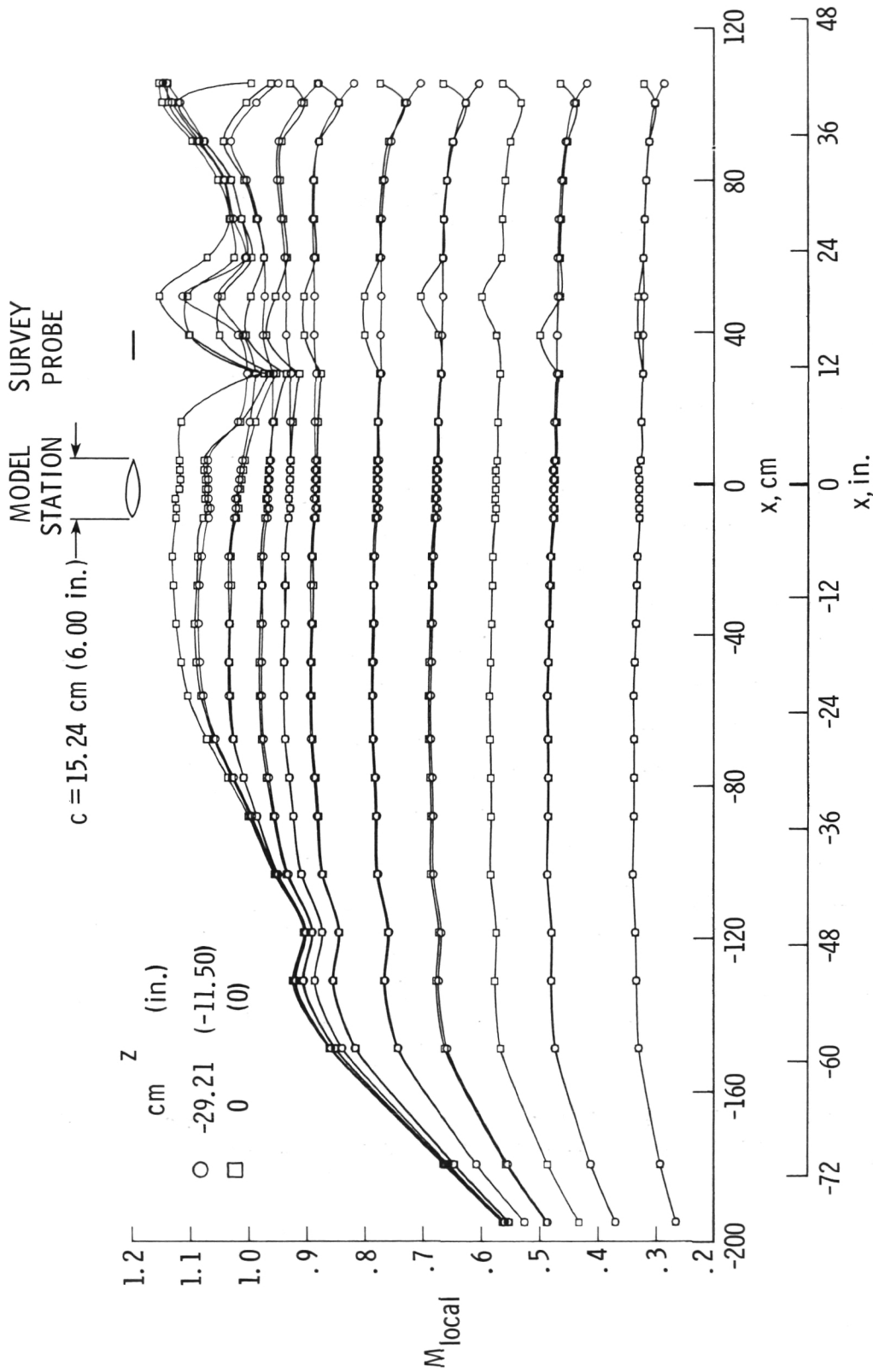
Figure 15.— Longitudinal sidewall Mach number distribution along $z = 7.62$ cm (3.00 in.). Flaps at 60 percent open; $p_{t,\infty} = 207$ kPa (30 psia); traversing survey probe at $z = 0$ and $z = -29.21$ cm (-11.50 in.).

33
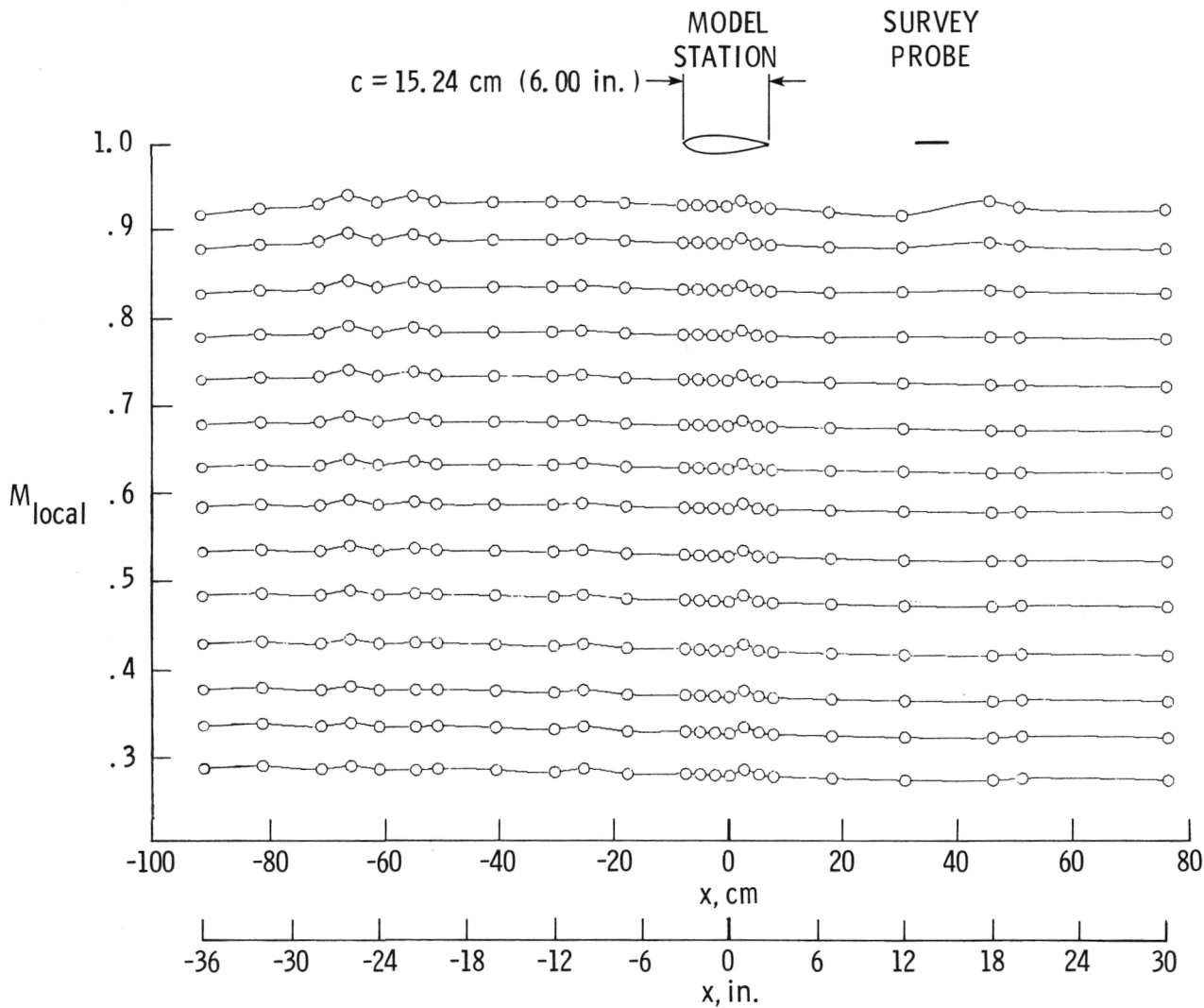
Figure 16.- Longitudinal sidewall Mach number distribution along $z = -7.62$ cm
(-3.00 in.). Flaps set according to M_{TC}; traversing survey probe at
$z = -29.21$ cm (-11.50 in.); $p_{t,\infty} = 207$ kPa (30 psia).
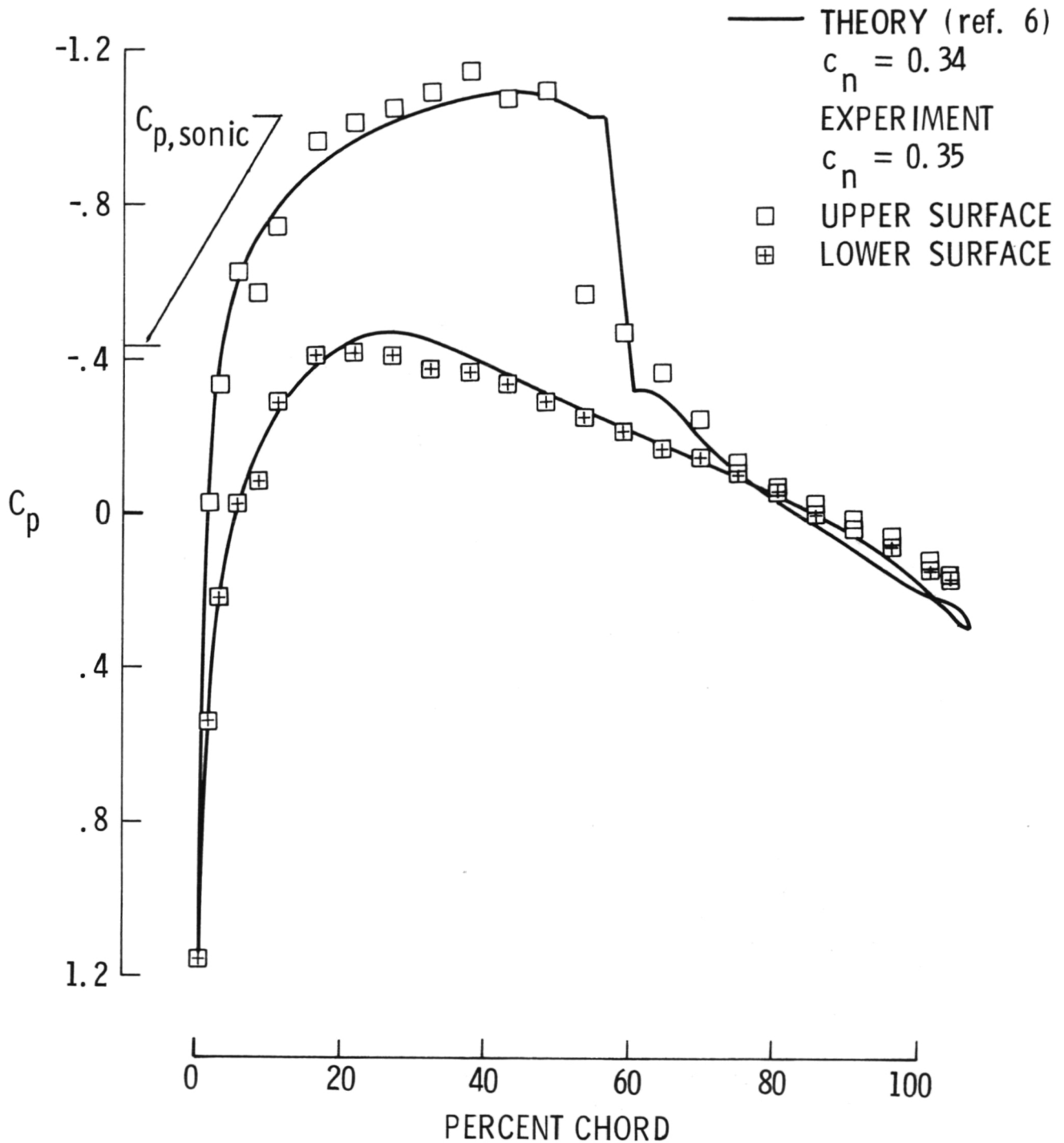
Figure 17.– Comparison of theoretical and experimental pressure distributions on NACA 0012 airfoil. $M_\infty = 0.800$; $R = 6 \times 10^6$; boundary-layer transition at 7.5 percent chord; plenum pressure used to determine free-stream Mach number for experimental data.
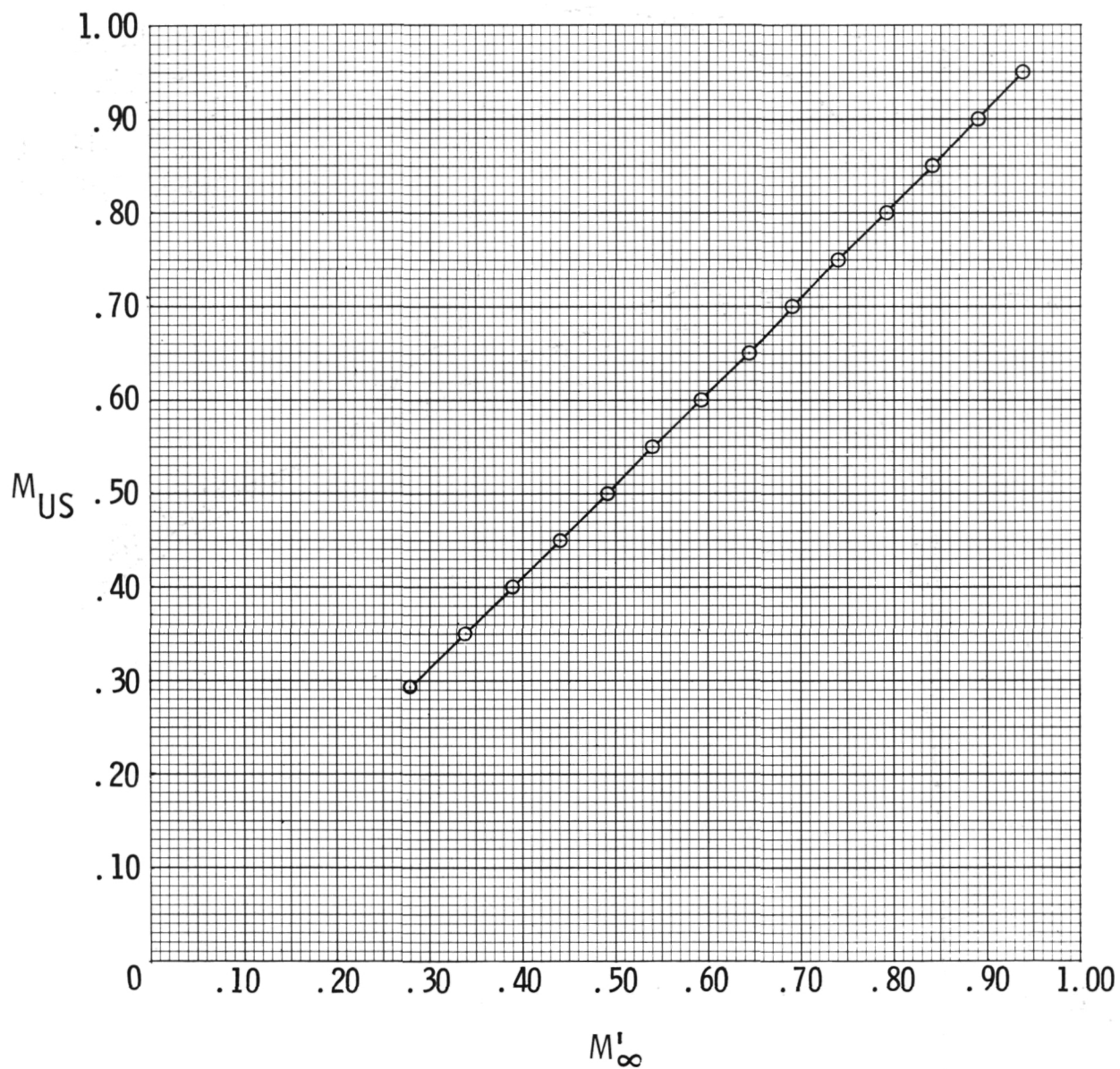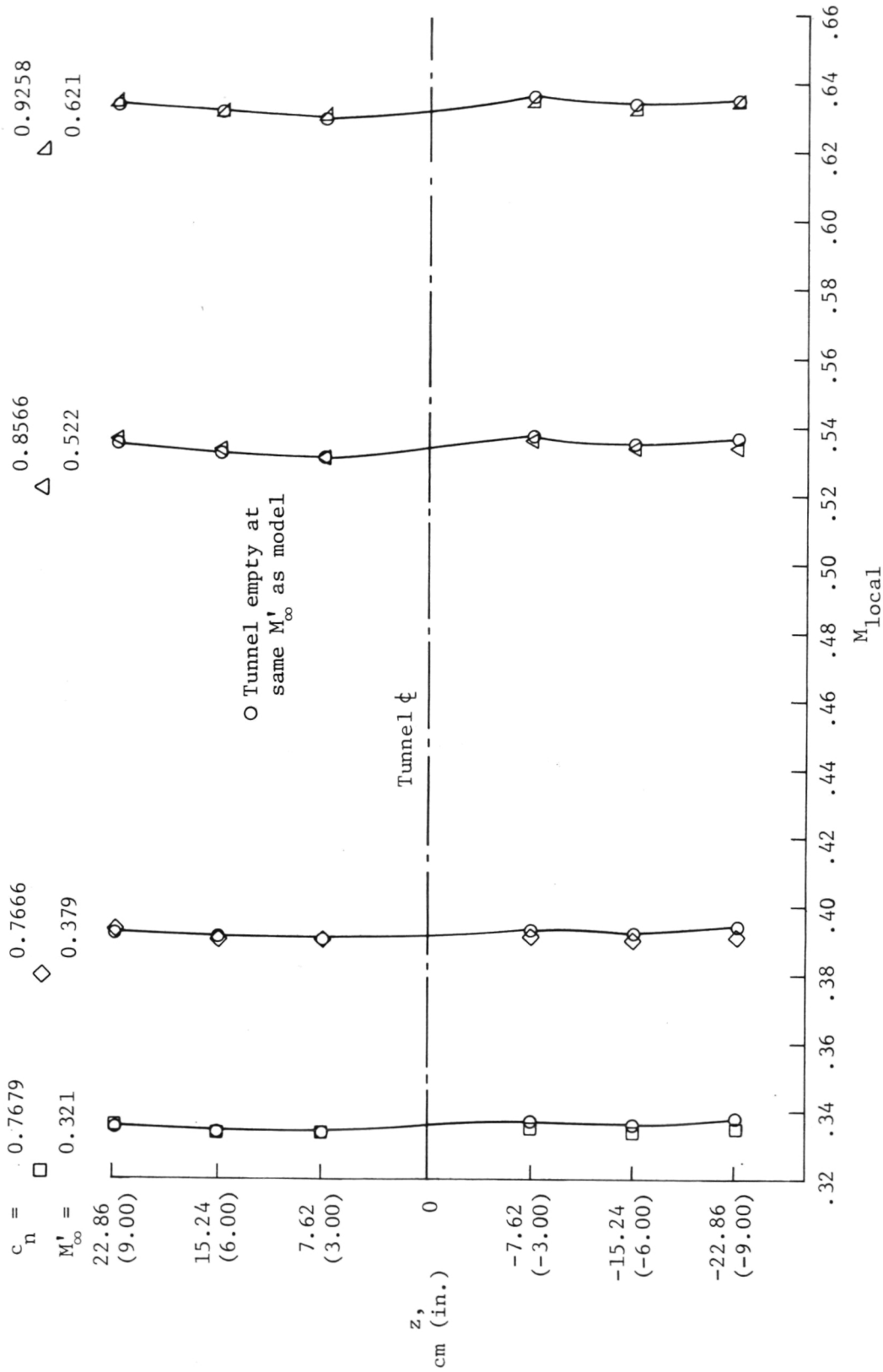
Figure 18.- Variation of upstream Mach number M_{US} at $x = -66.04$ cm
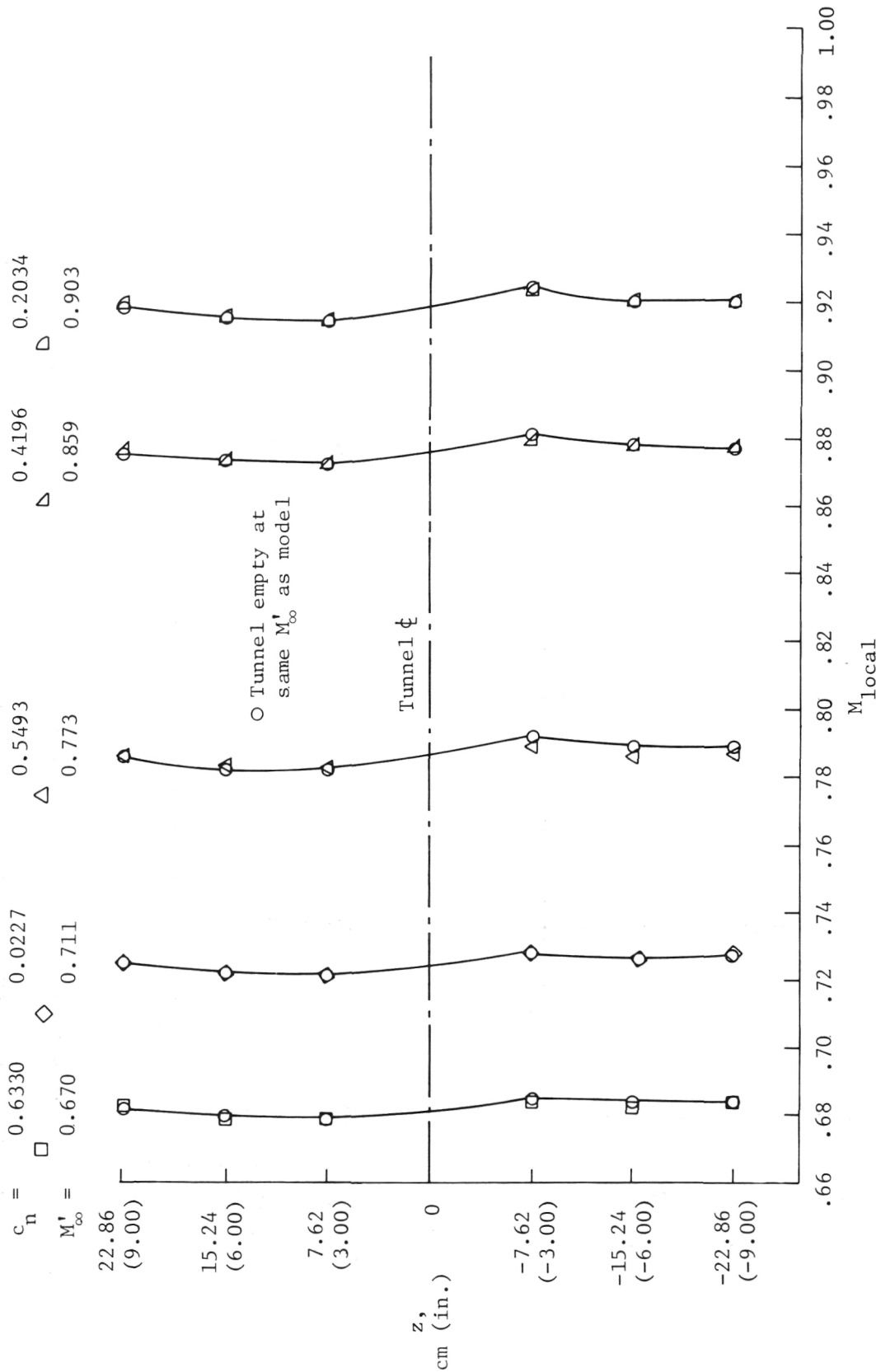(-26.00 in.) with Mach number at model station M'_∞.

(a) NACA 65_1-213, $a = 0.5$ airfoil model, $c = 20.32$ cm (8.00 in.).

Figure 19.- Effect of model lift on vertical upstream Mach number distribution measured at $x = -66.04$ cm (-26.00 in.).

(b) NACA 65_1-213, a = 0.5 airfoil model, c = 20.32 cm (8.00 in.) and NACA 0012 airfoil model, c = 15.24 cm (6.00 in.).
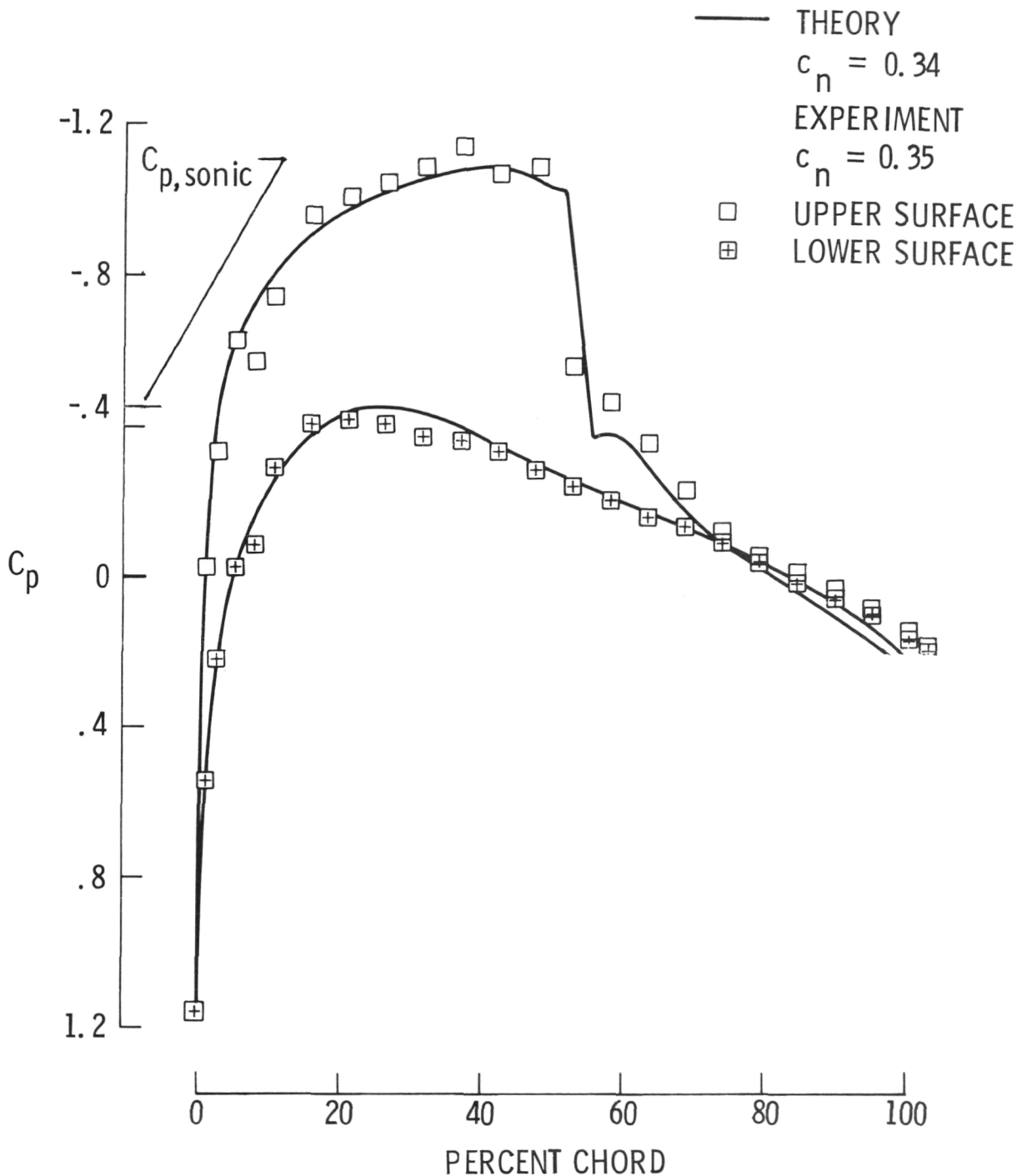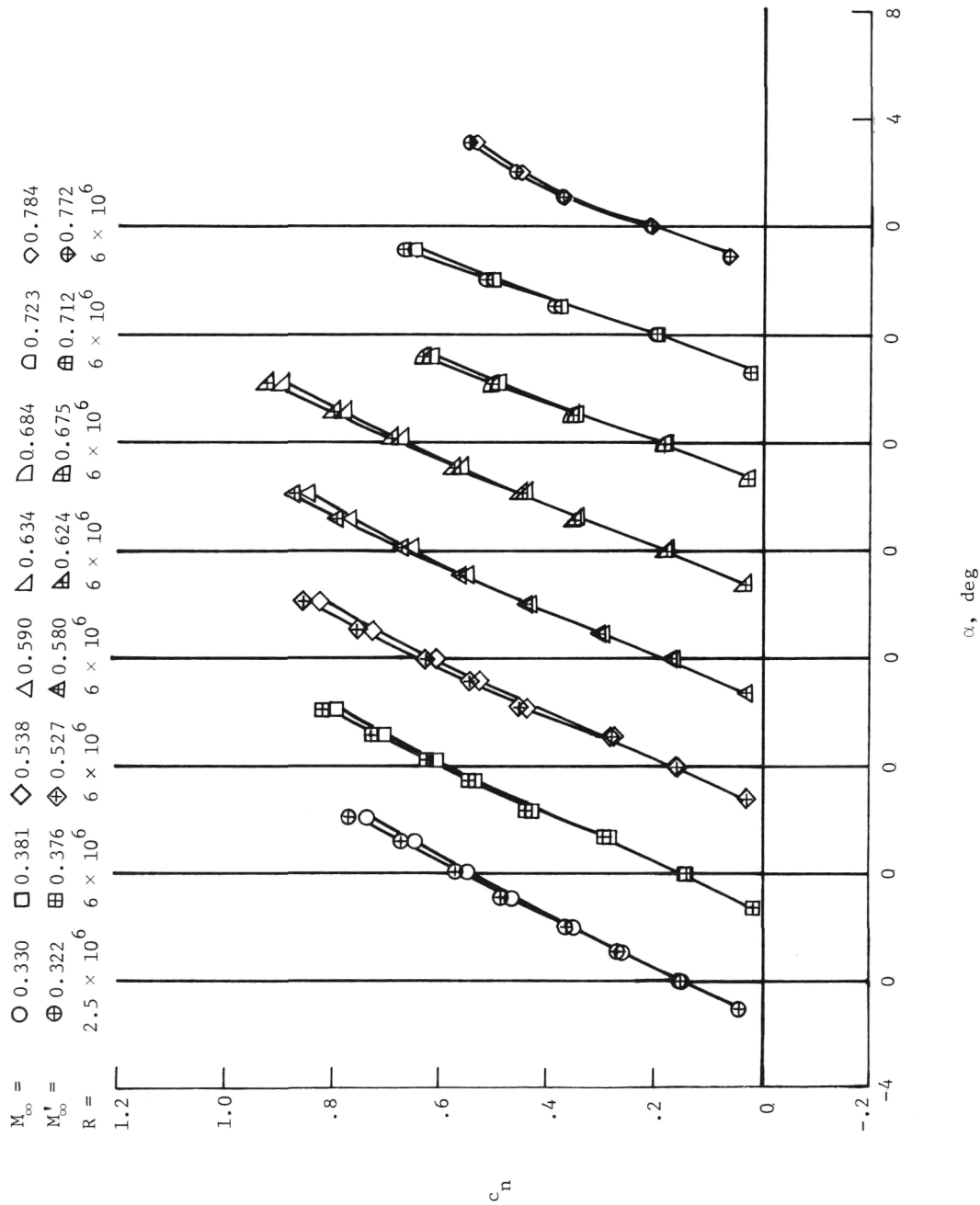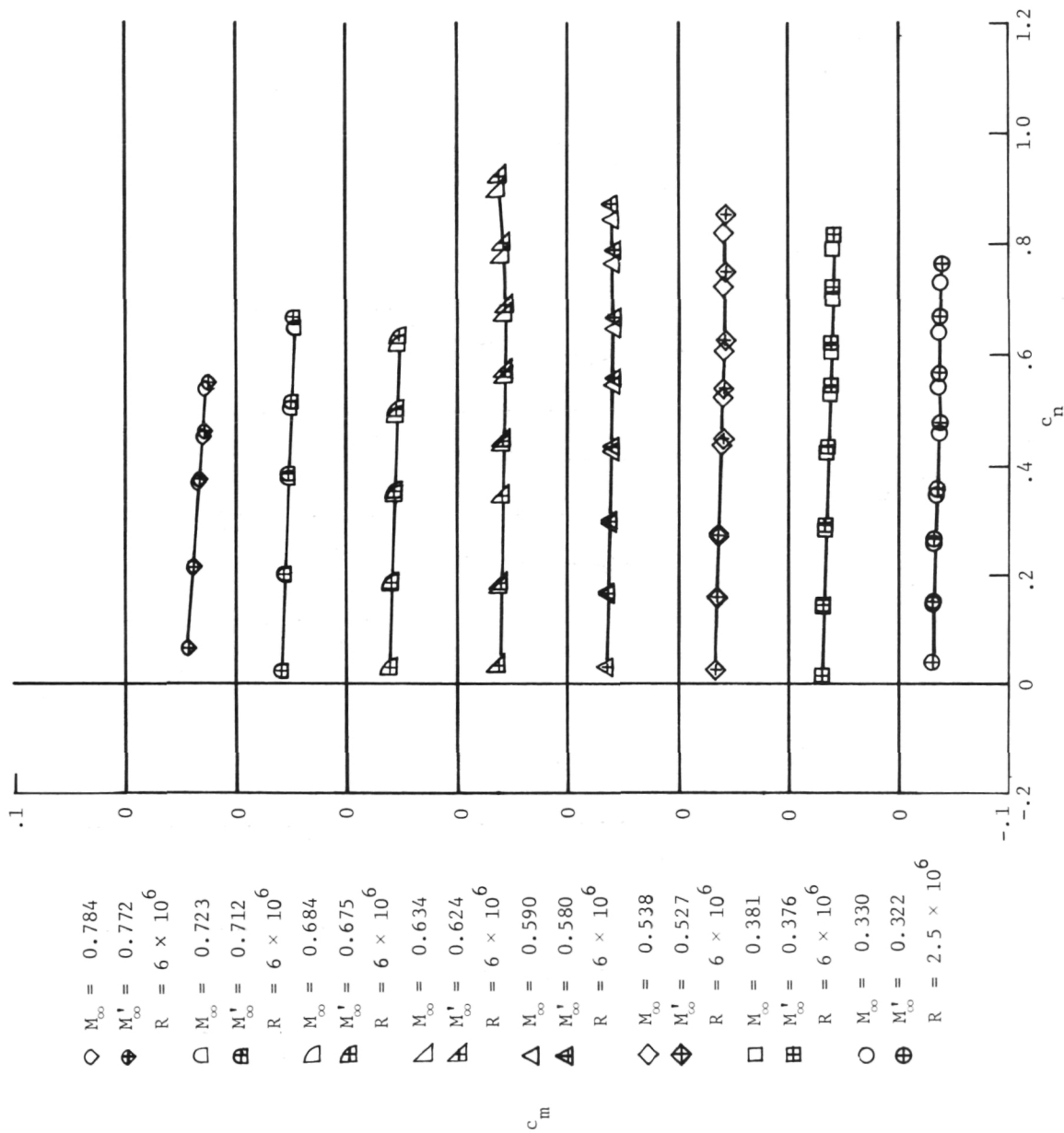
Figure 19.- Concluded.

Figure 20.- Comparison of theoretical and experimental pressure distribution on NACA 0012 airfoil. $M_\infty = 0.794$; $R = 6 \times 10^6$; boundary-layer transition at 7.5 percent chord; local Mach number 4.33 chords upstream of model used to determine free-stream Mach number for experimental data.
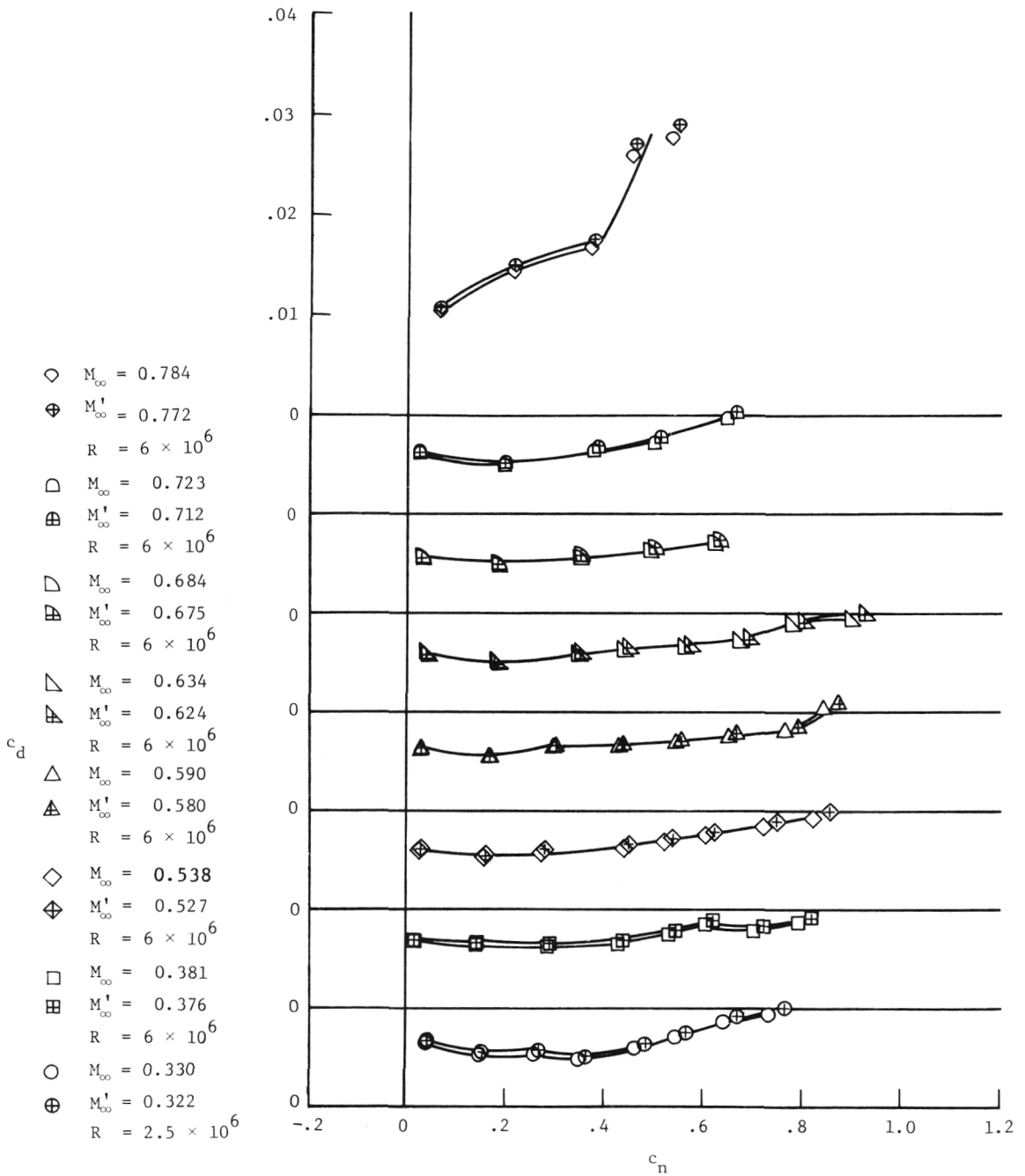
M_∞ =

M_∞' =

R =

○ 0.330 □ 0.381 ◇ 0.538 △ 0.590 △ 0.634 □ 0.684 □ 0.723 ◇ 0.784

⊕ 0.322 ⊞ 0.376 ⊕ 0.527 ▲ 0.580 ▲ 0.624 ▲ 0.675 ⊞ 0.712 ⊕ 0.772

2.5 × 10⁶ 6 × 10⁶ 6 × 10⁶ 6 × 10⁶ 6 × 10⁶ 6 × 10⁶ 6 × 10⁶ 6 × 10⁶

c_n

1.2

1.0

.8

.6

.4

.2

0

-.2

-4   0   0   0   0   0   0   0   4   8

α, deg

(a) Section normal-force coefficient.

Figure 21.- Aerodynamic characteristics of NACA 65₁-213, a = 0.5 airfoil measured in Langley 6- by 28-Inch Transonic Tunnel.

(b) Section pitching-moment coefficient.

Figure 21.- Continued.

(c) Section drag coefficient.

Figure 21.- Concluded.

1. Report No.	2. Government Accession No.	3. Recipient's Catalog No.
NASA TM-81947		

4. Title and Subtitle	5. Report Date
DESCRIPTION OF RECENT CHANGES IN THE LANGLEY 6- BY 28-INCH TRANSONIC TUNNEL	May 1981
	6. Performing Organization Code
	505-31-33-04

7. Author(s)	8. Performing Organization Report No.
William G. Sewall	L-13609
	10. Work Unit No.

9. Performing Organization Name and Address	11. Contract or Grant No.
NASA Langley Research Center Hampton, VA 23665	
	13. Type of Report and Period Covered

12. Sponsoring Agency Name and Address	Technical Memorandum
National Aeronautics and Space Administration Washington, DC 20546	14. Sponsoring Agency Code

15. Supplementary Notes

16. Abstract

Calibrations were obtained in the Langley 6- by 28-Inch Transonic Tunnel with newly installed controllable reentry flaps and test-section floor and ceiling. This study has indicated satisfactory tunnel-empty sidewall Mach number distributions using the controllable flaps with the new floor and ceiling. In addition, this study shows an improved Mach number calibration by using a pressure measured on the test-section sidewall upstream of the model rather than the plenum pressure in the chamber surrounding the test section.

17. Key Words (Suggested by Author(s))	18. Distribution Statement
Transonic tunnels Two-dimensional tunnels Wind-tunnel calibration Slotted-wall wind tunnels	Unclassified - Unlimited
	Subject Category 09

19. Security Classif. (of this report)	20. Security Classif. (of this page)	21. No. of Pages	22. Price
Unclassified	Unclassified	42	A03

National Aeronautics and
Space Administration

Washington, D.C.
20546

Official Business
Penalty for Private Use, $300

THIRD-CLASS BULK RATE

U.S.MAIL

NASA

POSTMASTER: If Undeliverable (Section 158
Postal Manual) Do Not Return

20 OCT 81 A.M   D. Chamberlain 254/103'/A3   18 JUL 84 UL

1 00   15 MAY REC'D